Mechanistic Study of the Formation of Bright White Light-Emitting Ultrasmall CdSe Nanocrystals: Role of Phosphine Free Selenium Precursors

Sukanta Dolai[1], Poulami Dutta,[2] Barry B. Muhoberac[1], Charles D. Irving,[1] and Rajesh Sardar[1,3] &

[1]Department of Chemistry and Chemical Biology, Indiana University-Purdue University Indianapolis, 402 N. Blackford Street, Indianapolis, Indiana, 46202, United States

[2]Department of Chemistry, Michigan State University, East Lansing, 578 South Shaw Lane, Michigan, 48824, United States

[3]Integrated Nanosystems Development Institute, Indiana University-Purdue University Indianapolis, 402 N. Blackford Street, Indianapolis, Indiana 46202, United States

This is the author's manuscript of the article published in final edited form as:
Dolai, S., Dutta, P., Muhoberac, B. B., Irving, C. D., & Sardar, R. (2015). Mechanistic Study of the Formation of Bright White Light-Emitting Ultrasmall CdSe Nanocrystals: Role of Phosphine Free Selenium Precursors. Chemistry of Materials, 27(3), 1057-1070. http://dx.doi.org/10.1021/cm5043638

ABSTRACT: We have designed a new non-phosphinated reaction pathway, which includes synthesis of a new, highly reactive Se-bridged organic species (chalcogenide precursor), to produce bright white light-emitting ultrasmall CdSe nanocrystals of high quality under mild reaction conditions. The detailed characterization of structural properties of the selenium precursor through combined ^{77}Se NMR and laser desorption ionization-mass spectrometry (LDI-MS) provided valuable insights into Se release and delineated the nanocrystal formation mechanism at the molecular level. The ^{1}H NMR study showed that the rate of disappearance of Se-precursor maintained a single-exponential decay with a rate constant of 2.3 x 10^{-4} s^{-1} at room temperature. Furthermore, the combination of LDI-MS and optical spectroscopy was used for the first time to deconvolute the formation mechanism of our bright white light-emitting nanocrystals, which demonstrated initial formation of a smaller key nanocrystal intermediate $(CdSe)_{19}$. Application of thermal driving force for destabilization resulted in $(CdSe)_n$ nanocrystal generation with n = 29-36 through continuous dissolution and addition of monomer onto existing nanocrystals while maintaining a *living-polymerization* type growth mode. Importantly, our ultrasmall CdSe nanocrystals displayed an unprecedentedly large fluorescence quantum yield of ~27% for this size regime (<2.0 nm diameter). These mixed oleylamine and cadmium benzoate ligand-coated CdSe nanocrystals showed a fluorescence lifetime of ~90 ns, a significantly large value for such small nanocrystals, which was due to delocalization of the exciton wavefunction into the ligand monolayer. We believe our findings will be relevant to formation of other metal chalcogenide nanocrystals through expansion of the understanding and manipulation of surface ligand chemistry, which together will allow the preparation of *"artificial solids"* with high charge conductivity and mobility for advanced solid-state device applications.

INTRODUCTION

Understanding the formation mechanism of semiconductor nanomaterials is fundamentally significant in that it will allow judicious control of their optical and electronic properties, which are important for applications in lasers,[1] photovoltaic cells,[2-4] and multi-colored light-emitting diodes (LEDs).[5-8] Recently, several studies were conducted to elucidate quantum dot (QD) formation,[9-11] specifically the mechanisms underlying the generation of monomers[12-14] from various metal and chalocogenide precursors. Almost all previous studies have exclusively used trialkylphosphine chalcogenides ($R_3P=E$; E= S, Se, Te) for the production of metal chalocogenide QDs, and from spectroscopic analysis it was proposed that *"magic-sized"* nanocrystals (MSNs) (<1.5 nm in diameter) are formed as key intermediates, which undergo further growth to form QDs.[15-18] Because of high reaction temperature, the appearance and disappearance of these intermediate nanocrystals were very rapid. Thus they have not been isolated and characterized, and even their structural properties remain elusive.

An in-depth understanding of the formation mechanism would allow the optimization of preparation of high-quality ultrasmall (1.5-2.0 nm diameter) semiconductor nanocrystals. In this context, ultrasmall nanocrystals have the ability to (1) serve as active precursors in the formation of various anisotropic nanostructures,[15,19-21] and (2) undergo fast charge separation and slow recombination.[22-24] Despite immense interest in ultrasmall nanocrystals in fundamental chemical processes, only a handful of high temperature[25-27] or alkylphosphine[28-29] precursor-based synthetic methods have been developed to prepare them. Very recently, low temperature, non-phosphinated methods for synthesis of ultrasmall CdSe nanocrystals were reported.[30-31] However, these synthetic methods have not answered the critical questions necessary to clearly understand the formation mechanisms of QDs involving MSNs. For example do "magic-sized" key

intermediates exist? What are their atomic compositions? What is (are) the chemical process(es) involved in their transformation into ultrasmall nanocrystals or QDs? To more fully understand the complex chemical phenomenon of nanocrystal or QD formation, it is important to investigate new experimental conditions and perhaps design new chalocogenide precursors, which together would allow *low temperature* synthesis and a reduction of reaction rate. This approach should allow us to isolate intermediate species and experimentally answer the question of the existence of magic-sized intermediates, and thus expand our understanding of the formation mechanism.

In order to address the current challenges of understanding the formation mechanism of semiconductor nanocrystals, we have investigated here the formation of ~1.6 nm CdSe nanocrystals using a new Se precursor (Scheme 1) prepared from a reaction between elemental selenium and 1-octadecene (ODE) requiring 1-hexanethiol (HT), which will be heretofore referred to as Se-ODE-HT. From ^{77}Se and ^{1}H NMR, and MS characterizations, we identify this Se-ODE-HT precursor as a new Se-bridged organic species that can be used in CdSe nanocrystals synthesis as the reactive Se precursor. Also for the first time we were able to isolate the key intermediate of a *"molecule-like"* $(CdSe)_{19}$ nanocrystal, which underwent a *"living-polymerization"* type growth at low temperature (60-100 ^{o}C) to form ultrasmall (~1.6 nm in diameter) CdSe nanocrystals. Importantly, these nanocrystals emitted bright white light and displayed photoluminescence (PL) quantum yield (PLQY) of up to 27%, which is the highest value known in the literature for this type of nanocrystal[26,32-33,34] formed through direct synthesis. An in-depth surface characterization has been performed to uncover the pivotal role of surface ligands in inducing such a large PLQY from this type of nanocrystal.

Taken together, the unique Se precursor we reported here will open new avenues of metal chalcogenide nanocrystals synthesis by enhancing the mechanistic understanding of

precursor evolution and conversion kinetics, as well as release of Se. Furthermore, the mild synthetic conditions will allow manipulation of the surface ligand chemistry through *in-situ* attachment to nanocrystals of various ligands that reduce nonradiative surface trap states and increase nanocrystals PLQY. The later is very important in the study of fundamental photophysical properties[35-38] of ultrasmall nanocrystals and in their potential use for fabrication of solid-state devices such as photovoltaic and light emitting diodes (LEDs). Our experimental results clearly demonstrate the importance of the reactivity of the chalocogenide precursor in the process of synthesizing high quality semiconductor nanocrystals under mild experimental conditions.

RESULTS AND DISCUSSION

The nanocrystals were synthesized according to Scheme 1 with detailed procedures for both precursor and nanocrystal syntheses provided in the experimental section. The CdSe nanocrystals prepared from (1) Cd(acetate)$_2$ and oleylamine (OLA), or (2) CdO, benzoic acid (BA), and OLA are designated as CdSe(OLA) and (CdSe)(BA/OLA), respectively. Briefly, nanocrystals were synthesized when Se-ODE-HT was swiftly injected into either of the cadmium precursors, incubated at room temperature for ~1 h, and then heated at 60 ^{o}C for either 24 (1, above) or 48 h (2, above), depending on the choice of cadmium precursor. The resulting nanocrystals were purified and characterized to determine their structural and photophysical properties. Prior to our nanocrystal synthesis we investigated the identity and reactivity of Se-ODE-HT and compared it with the Se-ODE precursor, which had been used in CdSe QDs synthesis by others [39-40] and will be discussed after addressing our CdSe nanocrystal synthesis.

Optical Characterization of Resulting White Light-Emitting CdSe Nanocrystals. Figure 1 represents the UV-vis and PL spectra of purified CdSe(OLA) and CdSe(BA/OLA) nanocrystals. Both kinds of nanocrystals displayed their lowest energy absorption peak position at 410 nm and a diameter of ~1.6 nm as determined from high-resolution transmission electron microscopy (HRTEM) (Figure S1). The emission spectra of both nanocrystals showed a combination of sharp band edge and then broad emission covering the entire visible region. The broad PL can be attributed to the trap state emission originating from various types of surface defects[12,26,41-42] as observed before for ultrasmall CdSe nanocrystals synthesized at higher temperature using a phosphine-containing selenium precursor.[34] The band edge emission was well-separated from the broad band emission with minimal overlap.

This sharp band-edge is a direct indication of the crystalline core of the nanocrystals whereas broad band emission is almost an exclusively surface-related phenomenon dictated by the surface ligand chemistry. Three important observation were made by a careful comparison of the optical spectra of CdSe(OLA) and CdSe(BA/OLA) nanocrystals: (1) The peak at 368 nm, which was assigned to the 1S(e)-$2S_{3/2}$(h) transition[43-44] was more pronounced with CdSe(BA/OLA) in comparison to only a shoulder in CdSe(OLA) nanocrystals. (2) The position of the broad emission band was shifted slightly to longer wavelength in CdSe(BA/OLA). (3) The intensity of the broad emission band (560-570 nm) was more intense relative to the band edge near 440 nm in CdSe(BA/OLA). These spectral observations strongly suggest that the surface ligand chemistry was different for CdSe(BA/OLA) and CdSe(OLA).

We hypothesize that the relatively pronounced 1S(e)-$2S_{3/2}$(h) transition of CdSe(BA/OLA) nanocrystals was due to their particular surface ligand chemistry with their stoichiometric core passivated with a mixture of OLA and $Cd(O_2CPh)_2$, whereas only OLA was

present as the surface passivating ligand for CdSe(OLA) nanocrystals. It is known that synthesis of QDs in the presence of anionic X-type ligands, e.g., the benzoate ion, results in surface metal cation rich nanocrystals to maintain the overall charge neutrality of ligand-coated QDs.[44-49] We believe that the existence of a similar atomic structure at the surface of our ultrasmall nanocrystals influenced the peak sharpness for 1S(e)-$2S_{3/2}$(h) transition, as was recently demonstrated for CdSe QDs.[44] The ~8 nm red shift in the broad emission band of our nanocrystals also indicates that their surface was composed of different ligands, which influenced exciton delocalization as will be discussed later. The insert in Figure 1A and B shows photographs of our white light emitting CdSe nanocrystal solutions illuminated at 365 nm at room temperature. The Commission Internationale d'Eclairage (CIE) chromaticity coordinates for CdSe(OLA) and CdSe(BA/OLA) nanocrystals are (x = 0.310, y = 0.316) and (x = 0.330, y = 0.337), respectively (Figure 1 B and D). Importantly the CIE coordinates for (CdSe)(BA/OLA) nanocrystals are almost identical to pure white-light as perceived by the naked eye (CIE coordinates; x = 0.333, y = 0.333). Based on this experimental result we believe that the surface structure of the ultrasmall nanocrystals or more precisely their surface ligand chemistry plays an important role in the color output of the emission. Previously, it was shown that the CIE coordinates of ultrasmall CdSe nanocrystals can be tuned by controlling the structure and mode of binding of surface ligands.[50] However, those CdSe nanocrystals reported so far displayed color in the yellow region in contrast to our nanocrystals, which displayed nearly pure white-light. Our article later provides extensive structural and photophysical characterization of Cd(OLA) and Cd(BA/OLA) nanocrystals along with various control experiments, which will provide a fundamentally new outlook concerning surface chemistry of ultrasmall nanocrystals.

Investigation of the Formation of White Light-Emitting CdSe Nanocrystals. Since the discovery of the hot injection method by Murray et al.,[51] a large number of synthetic protocols have been developed for preparation of high quality nanocrystals.[18,52-54] Such protocols are important to more fully understand their structural parameters (size, shape, composition, and surface surface ligand chemistry) and find application in optolectronic and photovoltaic device fabrication. Recently, exploration of mechanistic understanding of nanocrystal formation has been geared towards the goal of finding experimental conditions to prepare nanocrystals with controllable structural properties.[10,13-14,49] Peng et al. suggested that thermodynamically stable, ultrasmall nanocrystals also known as MSNs (display single-sized and homogeneous spectral line broadening),[25] are the key intermediates in formation of regular nanocrystals (RNCs) (display size distribution with either homogeneous or heterogeneous spectral line broadening).[15,55] Weiss and coworkers recently proposed "step growth" and "living" polymerization mechanisms in the preparation of CdSe QDs using ultrasmall nanocrystals as precursors at elevated temperature (>140 ^{0}C).[56] The literature describes detection of MSNs through optically during the high temperature synthesis of QDs, but never structurally isolated and characterized. This lack is because at high temperature, disappearance of MSNs and appearance of RNCs are extremely fast, and in most cases take place on the millisecond to second time scale. This leaves a large void in our understanding of the nanocrystal formation mechanism that apparently involves initial existence of MSNs as key intermediates[15] that were never experimentally characterized. Characterizing the structure of the intermediates and providing a mechanistic understanding of their transformation to RNCs may open new, cost effective synthetic methods for preparation of high quality nanomaterials (such as demonstrated in this article) yielding bright-white-light-emitting ultrasmall CdSe nanocrystals.

Now we show that the MSN $(CdSe)_{19}$, is the key intermediate for the preparation of RNCs at the temperature 60 ºC. Figure 2 illustrates the time-dependent formation of OLA-coated CdSe nanocrystal by UV-vis absorption spectroscopy. After injection of the Se-ODE-HT precursor into the Cd-OLA precursor at room temperature, a broad shoulder was slowly converted into two well-resolved peaks at 335 and 363 nm over the course of 1 h. The shifting of the band–edge absorption peak towards higher wavelength was correlated with the continuous but not the quantized growth model, as reported in the literature.[12,29,57] The position of the lowest energy absorption peak at ~360 nm suggests that our sample may contain MSNs of $(CdSe)_{19}$.[58] The peak position at 363 nm and intensity were stable for days at room temperature. Since MSNs have low chemical potential and are also found at a local minima in the size dependent solubility curve,[15] they can not overcome the thermodynamic stability barrier to form RNCs through the Gibbs-Thompson growth mechanism at low temperature.[53,59] Therefore, we believe that the thermodynamic stability of $(CdSe)_{19}$ at room temperature prevented the progression to RNCs. To confirm the identity of the CdSe nanocrystals and investigate the effects of surface ligand chemistry on the optical band gap, we purified samples withdrawn at one-hour time intervals, and analyzed the isolated product by LDI-MS (see Figure 2C). The spectrum shows a relatively broad peak centered at 3680.5 Da. We believe this is the mass of only the inorganic core without any surface passivating ligands. Previously our work[41] and that of the Buhro[60-61] group demonstrated that ligand detachment is a common problem in LDI-MS analysis, specifically when ligands (e.g., aliphatic amines) are datively-bound to the nanocrystal surface. Our X-ray photoelectron spectroscopy (XPS) and energy dispersive X-ray spectroscopy (EDS) analyses yielded the Cd/Se ratio of 1:1. Based on these two characterizations, we predicted that our sample contained $(CdSe)_{19}$ MSNs. The peak broadness could indicate that the sample does not

contain exclusively $(CdSe)_{19}$ nanocrystals but was highly enriched with that ratio. In the literature, existence of $(CdSe)_{19}$ has been discussed using theoretical calculations[58,62] and optical characterization.[21] Even though $(CdSe)_{13}$ and $(CdSe)_{33/34}$ nanocrystals were prepared in gram scale and isolated in almost pure form, to the best of our knowledge $(CdSe)_{19}$ nanocrystals have not been isolated yet. This lack could be due to their relatively low stability in comparison to other magic-sized nanocrystals such as $(CdSe)_{13}$ and $(CdSe)_{33/34}$.[60,63] It should be mentioned that the broadness of the LDI-MS peak (covering 5.5-7.5 kDa) could be due to formation of other MSNs during the laser ablation as had earlier been reported.[60]

Until now the literature have reported that exclusive formation of single-sized MSNs such as $(CdSe)_{13}$, $(CdSe)_{34}$, or $(CdSe)_{56}$ has only been observed at room temperature.[41,60,63] Upon heating these nanocrystals at moderately high temperature (>100 ^{0}C), RNCs were formed, which is due to destabilization of MSNs by overcoming the energy barrier. Figure 2B shows the UV-vis spectra of the our reaction mixture containing $(CdSe)_{19}$ nanocrystals at 60 ^{0}C. Interestingly, with time not only did the band-edge peak red-shift but also the peak intensity decrease. There are two possible scenarios that would reduce the absorption peak intensity: (1) complete decomposition of $(CdSe)_{19}$ nanocrystals into unreactive molecular species, and (2) converting a certain percentage of $(CdSe)_{19}$ nanocrystals into molecular species ("monomers"), which attached to the patent nanocrystals and grow via a living polymerization mechanism.[56]

Scheme 2 illustrates the proposed mechanism for formation of ultrasmall white-light emitting CdSe nanocrystals. In literature reports, synthesis of single-sized MSNs occurred at <40 ^{0}C,[29,41,60] whereas moderately high temperature (>120 ^{0}C) produced multiple families of MSNs[27-28] as well as RNCs.[18,27,53,64] Therefore, it remains unknown as to how the reaction temperature influences the structural reorganization of ultrasmall, parent MSNs into other MSNs or RNCs.

Through density functional theory (DFT) calculations, it was proposed that $(CdSe)_{19}$ nanocrystals possess a "core-cage" type structure.[58,63] Nucleophilic attack of the core-cage structure by free amines present in the reaction mixture can fragment the nanocrystals into monomers via ring opening, whereas fragmented $(CdSe)_{19}$ cores act as templates for formation of larger nanocrystals. Since the appearance of a new lower wavelength (340-360 nm) absorption peak was not observed, we ruled out the possibility of formation of $(CdSe)_m$ ($13 < m < 19$) in favor of formation of monomers. Based on our optical study, we believe that conversion of a certain percent of $(CdSe)_{19}$ nanocrystals into monomers would immediately reduce the overall nanocrystal concentration in solution (Step B2). However, we were unable to determine the fraction of $(CdSe)_{19}$ nanocrystals that underwent the fragmentation process. Nevertheless attachment of freshly generated monomers to the existing $(CdSe)_{19}$ nanocrystals promoted the red-shift due an increase in size (quantum confinement effect), but again overall nanocrystal concentration decreased (Step C and Step D). This process continued until all the monomers were consumed. We assume that the decreased absorption intensity was directly proportional to the nanocrystal concentration change given that the molar extinction coefficient (ε) is nearly constant. According to Mulvaney and coworkers, ε is nearly constant for CdSe nanocrystals having their band-edge absorption peak below 450 nm. Therefore, we believe that the decrease in UV-vis absorption peak intensity was due to the consumption of existing nanocrystals at the expense of the formation of larger nanocrystals.

To further elucidate our hypothesis in Scheme 2, we varied the RNC growth temperature. We expected that with increasing reaction temperature, the formation of larger nanocrystal would be faster but that the same path as observed at 60 ^{0}C would be maintained. Figure 3A illustrates the concentration versus time plot at three different reaction temperatures. As the

reaction temperature increased the thermal driving force for destabilization of $(CdSe)_{19}$ nanocrystals increased resulting in faster conversion of monomer as well as faster growth to $(CdSe)_n$ nanocrystals.

As shown in Figure 3B, initially the diameter of the nanocrystals increased linearly with time as evident of the living polymerization growth model proposed earlier.[56] Such a growth process produces nanocrystals with extremely low size inhomogeneity. However, there is a marked difference between previously proposed living-polymerization mechanisms and ours. We used alkylamine (OLA) as the surface passivating ligand in contrast to the long-chain fatty acid (oleic acid) used by Weiss and coworkers.[56] The authors observed that only anionic surfactants led to the proposed living polymerization mechanism. Importantly, in our system, similar time-dependent absorption characteristics were observed not only with OLA as the sole surfactant, but also when the CdSe nanocrystals were synthesized using benzoate ($-O_2CPh$) and OLA as the surfactant mixture. Therefore, we believe that formation of RNCs by the living-polymerization mechanism is controlled by both the chemical constituents and the stability of the intermediate species, but not by the chemical nature of the surfactants.

Our proposed mechanism (Scheme 2) of monomer formation from $(CdSe)_{19}$ nanocrystals is similar to what was previously reported by Strouss and coworkers[65] where MSNs were decomposed by hexadecylamine (~60 ^{0}C) and the fragmented clusters underwent structural reorganization to stable QDs. In our investigation, size focusing and existence of nearly monodispersed, fully grown CdSe nanocrystals also indicates that the formation process did not follow Ostwald ripening growth (i.e., defocusing and broad size distribution), but rather maintained a diffusion-controlled process (size-focusing)[55,57,59] as a form of the living-polymerzation model.

To further elucidate our proposed mechanism (Scheme 2) we performed the following control experiment. The OLA-coated $(CdSe)_{19}$ nanocrystals were synthesized at room temperature and purified using the procedure described in the experimental section. Entire isolated nanocrystals were dissolved in 3-mL of OLA and 2-mL ODE to reconstitute the original reaction condition and transferred to a pre-heated oil bath at 60 ^{0}C. Figure S2 shows the time dependent absorption spectra, which followed a very similar path as observed for our *in-situ* synthesis characterized by Figure 2B. Furthermore, the Ostwald-ripenning mechanism can be completely discounted since no additional cadmium or selenium precursors were added during our *ex-situ* control experiment. Based on our experimental evidence we believe that conversion of thermodynamically stable ultrasmall nanocrystals to other MSNs or RNCs depends on the structure and stability of the parent nanocrystals rather than the chemical nature of the surfactants. Nevertheless, our current formation mechanism that produces bright-white-light-emitting ultrasmall CdSe nanocrystals from compositionally well-defined key intermediate nanocrystal cores will open up new avenues for preparation of high quality nanocrystals with controllable size and core composition. Formation of key intermediates should depend both on (1) the monomer formation (Step A) and (2) nucleation and growth as described in the Lamer model,[10] where reactivity of the chalcogenide precursor plays the most critical role.[13-14] Therefore, it is of paramount interest to design and characterize new precursors that will expedite our understanding of nanocrystals formation and lead to the preparation of high quality nanomaterials.

Characterization of Se-ODE-HT Precursor. During last two decades, formation of metal chalcogenide QDs has been investigated using various trialkylphosphine chalcogenides (R_3P=E; E= S, Se, Te) as precursors.[13-14,29,49,66-68] In this context, the chemical identity of an important

selenium precursor, which is prepared by dissolving elemental selenium in ODE at high temperature (>180 ^{o}C) and used frequently in CdSe QD synthesis[40,52,69-71] has not been resolved. Several mechanisms have been proposed to explain the high temperature (>180 ^{0}C) preparation of the Se-ODE precursor with two shown in Scheme 3 (paths (i) and (ii)). The resulting Se precursors contain a large number of cross-linked species that include material with multiple Se-Se bonds, as reported previously from ^{77}Se NMR analysis[39] and also by an independent analysis by our group as shown in Figure 4. It was also reported[72] that heating elemental selenium in the presence of ODE at >220 ^{0}C produced a Se-bridged organic compound (Scheme 3, path (ii)), however at this temperature elemental selenium and monoolefins (e.g., ODE) undergo a vulcanization process and produce cross-linked species (path (i)).[39] Most noticeably, we have observed a distinct difference in reactivity during CdSe nanocrystal formation between the routinely used Se-ODE precursor (synthesized by reacting elemental Se with ODE at 180 ^{o}C for 2h) and our Se-ODE-HT precursor. As mentioned above, we were able to synthesize $(CdSe)_{19}$ nanocrystal-coated with either OLA or a mixture of BA/OLA at room temperature when Se-ODE-HT precursor was used. In this context, under identical experimental conditions, the Se-ODE precursor failed to produce any CdSe nanocrystals even after 24 h of stirring at room temperature (see Figure S3).

In order to determine the origin of higher reactivity, we characterized the chemical identity of our Se-ODE-HT precursor by ^{1}H and ^{77}Se NMR spectroscopy and MS. The ^{1}H NMR spectrum showed multiplets at ~5.4 ppm (Figure S4), indicating the formation of a new species, but we were unable to determine its chemical formula from the proton spectrum. Interestingly, as illustrated in Figure 4, the ^{77}Se NMR spectrum showed a single peak at ~600 ppm as opposed to several peaks ranging from 200-700 ppm present in Se-ODE precursor. The single peak at ~600

ppm in ^{77}Se NMR spectrum strongly suggests that our Se-ODE-HT precursor contained the Se-bridged organic species C as shown in Scheme 3, path (iii).[73] Additionally, from the ^{77}Se NMR analysis we can eliminate the possibility of formation of either crown ethers containing Se or polyselenoethers as shown in Scheme 3, path (ii). In such cases chemical shifts ranging from ~150 to 750 ppm should be observed.[73] Furthermore, from the NMR analysis, formation of a R-HC=Se compound can also be eliminated because the chemical shifts for ^{77}Se in seleno-carbonyl compounds appear between 170-220 ppm as observed for selenourea (218 ppm).[73] A parallel reaction was conducted to further explore the chemical structure of species C by producing a compound that closely resembles it. This selenium compound was prepared using (1) 2,4,6-trimethylstyrene (monoolefin) instead of ODE in the presence of HT and (2) identical mole ratios of reagents as used for the Se-ODE-HT precursor synthesis. When the new compound was characterized by ^{77}Se NMR, the spectrum showed a single peak at ~690 ppm (Figure 4). The slight downfield shift of the chemical resonance in ^{77}Se NMR spectrum in comparison to the Se-ODE-HT was likely from the highly conjugated benzene ring. In conjunction with ^{77}Se NMR identification of species C, we assign the multiple at ~5.4 ppm in ^{1}H NMR spectrum as the formation of a new Se-bridged organic species.

Taken together, we believe path (iii) summarizes the formation of our Se-bridged organic species C, which involves reduction of elemental selenium to Se^{2-} by thiols and then reactive Se^{2-} undergoing nucleophilic adduct formation with the olefin. It was reported that selenium powder can be reduced by thiols which oxidized to disulfide.[74] Indeed GC-MS analysis confirmed the formation of dihexyl-disulfide (*m/z* = 234) resulting from oxidation of HTs (Figure S5). A detailed discussion related to GC-MS data and further control experiments are provided in the Supporting Information File. The XPS (Figure S6) and EDS (Figure S7) analyses confirmed that

no residual sulfur-containing compounds were attached onto the surface of CdSe nanocrystals. Our experiment strongly supports our hypothesis that species C is formed through path (iii). The higher reactivity of our selenium precursor in comparison to Se-ODE described in the literature could be due to strain present in the three-member cyclic ring bridging the selenium, which could undergo facile selenium release as discussed next.

The Se-ODE-HT precursor isolated here and used for nanocrystal synthesis has provided five important features that contrast both Se-ODE and trialkylphosphine chalcogenide precursors commonly used in semiconductor nanocrystals synthesis. Firstly, the precursor can be prepared at temperature <160 ^{0}C, whereas the Se-ODE precursor required 180-250 ^{0}C. Secondly, the Se-ODE-HT precursor retains its reactivity even 4 days after preparation if stored under nitrogen as no change in the CdSe nanocrystal yield was observed (data not shown) but the Se-ODE precursor loses its reactivity within couple of hours after preparation.[39] Thirdly, only species C is present in the Se-ODE-HT precursor in comparison to several high to low molecular weight (cross-linked) species in the Se-ODE precursor. Fourthly, high quality CdSe nanocrystals can be synthesized using the Se-ODE-HT precursor at room temperature whereas such strong reactivity of Se-ODE has not yet been demonstrated. Finally and most importantly, appropriate reactivity of the Se-precursor provided the opportunity to synthesize and isolate a key intermediate to unravel the formation mechanism of RNCs for the first time.

^{1}H NMR Studies of Selenium-Release Kinetics. High quality MSN or RNCs can be prepared by controlling the reactivity of chalocogenide precursor and the rate of selenium release. Together these determine monomer concentration and influence nucleation and growth. Several studies were performed to investigate the release of selenium in synthesis of CdSe QDs[13-14] and

ultrasmall CdSe nanocrystals[29] in which trialkylphosphine selenides were used. Herein, for the first time we investigated the kinetics of selenium release in a nonphosphinated system through monitoring ^{1}H NMR. The previously discussed chemical structure of our selenium precursor is shown in Scheme 3 (species C), which shows multiplets at ~5.4 ppm. We hypothesize that the release of Se from species C would restore the double bond of the ODE. To prove this hypothesis, the CdSe nanocrystal synthesis was carried out in the presence of decylamine (DA) instead of OLA and Cd(acetate)$_2$. This choice was because in a crude reaction mixture the position of vinylic protons of OLA (m, 5.32-5.38 ppm) interferes with the proton signal originating from the Se-ODE-HT precursor at ~5.4 ppm. The crude reaction mixture was diluted with *chloroform-d* to quench the nanocrystal growth and then ^{1}H NMR spectra were acquired at regular intervals, as shown in Figure 5A. The peak associated with species C at ~5.4 ppm slowly diminished while the intensity of the peaks assigned to the allylic protons of ODE slowly increased. The chemical structure of the Cd precursor, which was prepared in the presence of alkylamine and carboxylic acid-containing ligands, is well established.[13-14,29] Based on literature reports and the reappearance of the allylic protons of ODE in our ^{1}H NMR spectra, we proposed Scheme 4 as the possible mechanism for Se release. We believe the release of selenium is a single step process where selenium directly attacks the activated cadmium precursor, and is unlikely by a two or multistep process as described recently.[13,67] Furthermore, the selenium was delivered as Se^{2-} and the cadmium center remained Cd^{2+}. The rate of disappearance of species C was also studied by monitoring the multiplets at ~5.4 ppm using ^{1}H NMR (Figure 5B). The decay of Se-ODE-HT was a single-exponential and the corresponding k_{obs} was $2.3 \pm 0.18 \times 10^{-4}$ s^{-1}. The release of selenium in our Se-ODE-HT precursor was nearly 10-fold slower than previously reported for the TOPSe precursor in CdSe QD synthesis.[13] However, CdSe QDs were

synthesized at 270 ^{o}C whereas our synthesis was performed at room temperature. We believe this new Se-bridged organic precursor will open up new avenues in the study of nanocrystal formation by providing a more mechanistic understanding of precursor evolution and release of Se, as is currently under further investigation.

Fluorescence Lifetime Measurement of White Light-Emitting CdSe Nanocrystals. Photophysical properties of QDs that are controlled by surface passivating ligands are well studied. However, scientific characterization of such properties for ultrasmall nanocrystals is not only limited, but also ambiguous.[27,34,37,75] Herein, we provide an in-depth structural characterization of ultrasmall CdSe nanocrystals and emphasize the important of surface ligand chemistry to achieve high PLQY and long fluorescence lifetime. The PLQYs of the CdSe(OLA) and CdSe(BA/OLA) nanocrystals were determined to be 11.2 and 26.9 %, respectively, using Coumarin-30 in acetonitrile (PLQY = 55.3 %) as the standard.[76] An ~27% PLQY is the highest value achieved for single-component, white light-emitting ultrasmall CdSe nanocrystals without any post-synthetic surface modification.[34] It is known that when semiconductor nanocrystals are synthesized in the presence of anionic surfactant, the resulting nanocrystals are metal rich. Therefore, we believe that in the case of CdSe(BA/OLA) nanocrystals, the surface contained $Cd(O_2CPh)_2$ as bound ligands to Se sites, whereas CdSe(OLA) nanocrystals were coated with OLA alone, which only binds to cadmium sites leaving the selenium sites unpassivated. The passivation of both surface cadmium and selenium sites would prevent the formation of charge trapping (hole) centers as well as stabilize the midgap states and increases PLQY.[35] Our experimental data nicely corroborate literature results which suggest that the presence of excess metal ions on the surface of the QDs increases the PLQY.[46,77]

In order to demonstrate the importance of surface ligand chemistry we now show that the presence of an excess $Cd(O_2CPh)_2$ layer on the CdSe nanocrystal surface can increase the PLQY. A control experiment was performed where CdSe(OLA) nanocrystals were synthesized, purified, and dissolved in toluene, followed by addition of solid $Cd(O_2CPh)_2$. Since $Cd(O_2CPh)_2$ is insoluble in toluene, the biphasic reaction mixture was stirred at room temperature. Over time, small aliquots of the reaction mixture were withdrawn and centrifuged to remove undissolved solid. The supernatants were analyzed by UV-vis and PL spectroscopy. Figure S8A illustrates the time dependence of the PLQY of CdSe(OLA) nanocrystals upon treatment with $Cd(O_2CPh)_2$. As expected, the PLQY measured by excitation at 380 nm increased nearly two fold as more $Cd(O_2CPh)_2$ attached to the surface of the nanocrystals without any noticeable shift in the lowest energy absorption band. The FT-IR spectrum confirmed the attachment of $Cd(O_2CPh)_2$ onto the CdSe nanocrystal surface (data not shown).

As mentioned above, the photophysical properties of ultrasmall nanocrystals can be significantly affected by their surface ligand chemistry. In this context, it is expected that the PL lifetime of the CdSe(OLA) and CdSe(BA/OLA) nanocrystals would be different. Figure 6 illustrates typical PL decays and their fitted curves, obtained using a time-correlated single photon counting (TCSPC) spectrophotometer. We found that the decay process of our ultrasmall CdSe nanocrystals has nonexponential decay dynamics, which can be fitted with a stretched exponential function (see experimental section, Eq. 2).[78] The black and blue curves represent the decay monitored at 440 and 550 nm, respectively. The lifetimes were determined to be 5.5 ± 1.0 ns (440 nm) and 38.2 ± 5.2 ns (550 nm) for the CdSe(OLA) nanocrystals, and 25.6 ± 3.0 ns (440 nm) and 80.5 ± 4.9 ns (550 nm) for the CdSe(BA/OLA) nanocrystals. The lifetime observed for CdSe(BA/OLA) nanocrystals is comparable to the literature value of 70 ns for 1.6 nm CdSe

nanocrystals passivated with a mixture of trioctylphosphine and trioctylphosphine oxide,[36] and nearly 30 fold larger than the literature reports of alkylamine-passivated ultrasmall CdSe nanocrystals.[25,29,41] Importantly, the trap-state lifetime for CdSe(BA/OLA) is two orders of magnitude larger than CdSe(OLA) nanocrystals. These data suggest that the radiative lifetime of bound excitons increases as a result of an increase in exciton confinement.

Based on the absorption peak position at 410 nm for both CdSe(BA/OLA) and CdSe(OLA) nanocrystals, we can assume that their inorganic core compositions are identical. Therefore, their variable surface ligand chemistry could be the determining factor for the observed differences in the lifetimes. It follows that a likely reason for the higher lifetime of CdSe(BA/OLA) nanocrystals is due to delocalization of the electron wave function into the ligand shell.[79] It was previously reported that surface passivating ligands can control exciton delocalization[80] and modulate photophysical properties and such effects are more profound for ultrasmall nanocrystals.[81] The trap state peak position of CdSe(BA/OLA) nanocrystal is red-shifted by 8 nm compared to CdSe(OLA) nanocrystal, which agrees with the literature [78-79] that electron delocalization results in a red-shift of the PL peak. In general, the photophysical properties of the ultrasmall CdSe nanocrystals are more complex than those of QDs. Ultrasmall nanocrystals have (1) a substantially larger surface-to-volume ratio than QDs and (2) the presence of a large number of surface occupied atoms, which together lead to the formation of trap states that are dominated by the interplay between crystal structure and surface ligand chemistry. Therefore, by selecting suitable surface ligands one could increase the probability of exciton delocalization and maximize the PLQY and lifetime.

Structural Characterization of CdSe Nanocrystals. Purified CdSe(OLA) and CdSe(BA/OLA) nanocrystals were analyzed by XPS, NMR, FT-IR, and LDI-MS to characterize their core and surface atomic compositions and further elucidate our hypothesis that surface ligand chemistry is playing an important role in high PLQY, as well as in producing the sharper 1S(e)-$2S_{3/2}$(h) electronic transition observed in Cd(BA/OLA) versus CdSe(OLA) nanocrystals. The XPS analysis of CdSe(OLA) nanocrystals showed 1.02 ratio for Cd/Se. The FT-IR analysis (Figure S9) demonstrated that no residual acetate ions or adsorbed water were present on the nanocrystal surface and it was coated almost exclusively with OLA. Our experimental data are in agreement with the literature that ultrasmall CdSe nanocrystals synthesized in the presence of alkylamines and $Cd(acetate)_2$ produced a stiochiometric core, which is coated with only amines.[41,60]

The CdSe(BA/OLA) nanocrystals were analyzed by FT-IR to acquire additional structural information concerning the nature of the bond between $–O_2CPh$ and the surface cadmium ions, (see Figure 7A). The symmetric and antisymmatric CO stretches are at 1387 and 1543 cm^{-1}, respectively and the separation between these two vibration modes of 156 cm^{-1} suggests that the $–O_2CPh$ ions are chemisorbed to the surface Cd ion through a bidentate interation.[29,44] Figure 7B represents the ^1H NMR spectrum of CdSe(BA/OLA) nanocrystals detailed as follows: broad aliphatic proton signals of OLA centered at 0.87 ppm (terminal $–CH_3$), 1.26 ppm ($– (CH_2)_{11}–$), 1.51 ppm ($–CH_2–CH_2–NH_2$), 2.00 ppm ($–CH_2–CH=CH–CH_2–$), and 2.78 ppm ($–CH_2–CH_2–NH_2$), as well as vinyl protons at 5.36 ppm ($–CH=CH–$) and three broad aromatic protons signals at 7.31 ppm, 7.39 ppm and 8.05 ppm, which are assigned as *meta*-, *para*- and *ortho*- protons, respectively. We believe that these nanocrystals contained a stoichiometric inorganic core and excess metal ions, in the form of Z-type ligand that are residing on the surface. Therefore, the CdSe(BA/OLA) nanocrystal surface was coated with a

mixed ligand coating with OLA and $Cd(O_2CPh)_2$ bound to the Cd and Se sites, respectively, which are part of the nanocrystal lattice as illustrated in Figure 7C.[77] Based on the above spectroscopic characterization we suggest that the passivation of both Cd and Se sites stabilizes the high-energy filled orbitals and charge trapping midgap states of CdSe(BA/OLA) nanocrystals, which resulted in an unprecedentedly large PLQY and long PL decay time for such ultrasmall semiconductor nanocrystals.[26-29,37,41,60,63,75,82] Therefore, finding suitable surface passivating ligands that can both bind to the surface metal and chalocogenide is of paramount interest in the context of the application of ultrasmall semiconductor nanocrystals in the fabrication of efficient solid-state devices.[3,7]

The precise characterization of the inorganic core composition of ultrasmall nanocrystals still remains a challenge, specifically those that emit white light.[26,34,83] There are recent literature reports demonstrating that LDI-MS analysis is a powerful technique to determine the core mass of ultrasmall CdSe nanocrystals.[41,60,63] Our OLA-coated and mixed OLA- and $Cd(O_2CPh)_2$-coated nanocrystals were characterized by LDI-MS as illustrated in Figure 8A. Analysis showed that our white-light-emitting CdSe nanocrystals do not contain a single size core but rather were composed of several very similar masses. The average core mass (m/z) was found to be 6315 for OLA-coated CdSe nanocrystals, which can be assigned to a stoichiometric core composition of $(CdSe)_{33}$ (calculated m/z = 6314.7) because XPS and EDS analyses confirmed their nearly 1:1 Cd:Se ratio. However, we were unable to determine the total molecular weight of the ligand-protected nanocrystals because complete ligand detachment was observed during the LDI-MS analysis as had been observed before for alkylamine-protected CdSe nanocrystals[41,60] and QDs.[84] The Gaussian fit of the acquired LDI-MS spectrum indicated that the CdSe nanocrystals were composed of species with mass (m/z) ranging from 5550 to 6890, which corresponds to $(CdSe)_{29}$

(cal. m/z = 5549.8) to $(CdSe)_{36}$ (cal. *m/z* = 6889.5). Importantly, mixed OLA- and $Cd(O_2CPh)_2$-capped CdSe nanocrystals showed an almost identical average core mass (*m/z)* of 6314.7, which can only be possible if the nanocrystals possessed a stoichiometric core with a layer of loosely bound $Cd(O_2CPh)_2$ complex on their surface. Interestingly, the Cd/Se ratio for the CdSe(BA/OLA) nanocrystals from the XPS analysis (Figure S10) was found to be 1.33 ± 0.01, and this value is close to the ratio of 1.29 ± 0.03 determined from EDS analysis. A recent study has indeed showed that the $Cd(O_2CPh)_2$ type complex (Z-type ligand) is very facile and easily undergoes ligand exchange reactions with other types of ligands (L- or X-type).[77] Therefore, we believe that during laser ablation in the LDI-MS analysis, both the surface bound OLA and $Cd(O_2CPh)_2$ were detached from the nanocrystal surface leaving stiochiometric cores. In the LDI-MS analysis, both types of CdSe nanocrystals exhibited a few other low intensity peaks correspond to $(CdSe)_{15}$, $(CdSe)_{16}$, $(CdSe)_{19}$, and $(CdSe)_{22}$, which were due to fragmentation of the $(CdSe)_n$ nanocrystal core. Importantly, the fragmentation pattern was different than bulk semiconductor CdSe, which only showed formation of $(CdSe)_{19}$ and $(CdSe)_{13}$ nanocrystals.[63] The difference in fragmentation pattern between bulk and nanocrystalline CdSe strongly suggests that our sample contained stiochiometric cores of $(CdSe)_n$ [n = 29-36] and not the artifacts in the LDI-MS analysis mentioned in recent literature.[56]

We believe this MS technique is a very appropriate analytical method for nanocrystal molecular weight determination. It has not only been used to characterize biological samples[85-86] but also heavily used to characterize ligand-protected metal nanoparticles.[87-88] However, there is controversy in the literature concerning the solution stability and composition of ultrasmall semiconductor nanocrystals and their core mass determined by LDI-MS.[56] It has been suggested that laser irradiation can result in dissociation of larger nanocrystals into smaller,

thermodynamically stable MSNs that exist in the gas phase, and therefore peaks which closely resembled MSNs are in reality artifacts of the ionization process and do not represent the actual core mass that exists in solution. This controversy arises because of the identical mass distribution and fragmentation pattern from both ultrasmall semiconductor nanocrystals and bulk semiconductor that had been observed in LDI-MS analysis.[63] To further confirm our experimental data that the sample contained $(CdSe)_n$ [n = 29-36] and to distinguish the fragmented species from the original nanocrystal cores, LDI-MS analysis was conducted with variable laser power levels. This approach is very useful in the context of determining the parent core and the fragmented species as was demonstrated for ultrasmall gold nanoparticles[87] and CdSe nanocrystals.[41] It is expected that increasing the laser power would increase the intensity of the fragmented species while decreasing the intensity of the original nanocrystal core. The LDI-MS spectra of mixed OLA- and $Cd(O_2CPh)_2$-coated CdSe nanocrystals at variable laser power levels is shown in Figure 8B. It is clearly evident that the intensity of the peak with an average *m/z* of 6315 decreased rapidly with increasing laser ablation and vanished completely, while the intensity of the peaks in the lower mass range increased and became more visible and defined. The increase of observed peak intensities below a mass of ~ 5000 as the laser power was increased clearly differentiated the fragments from the nanocrystal cores with masses in the range of 5500-6900. Thus, the MS analysis suggested that the difference in the absorption and PL properties between OLA-coated and mixed OLA- and $Cd(O_2CPh)_2$-coated ultrasmall CdSe nanocrystals was not due to the difference in their core composition, but rather was solely because of their surface ligand environment due to the physicochemical interaction between the stoichiometric CdSe core and surface passivating ligands.

Conclusion

In conclusion, we have demonstrated the utility of a new non-phosphinated Se-precursor-based synthetic approach to prepare high quality, bright white light-emitting ultrasmall CdSe nanocrytals. The ^{1}H and ^{77}Se NMR, and MS analyses confirmed existence of the new Se-bridged organic species. The ^{1}H NMR study showed that the rate of disappearance of selenium precursor maintain a single-exponential decay with a rate constant of 2.3×10^{-4} s^{-1} which is significantly higher than tose measured for alkylphosphine precursors. Our low temperature procedure allowed the appropriate reactivity to isolate nearly monodispersed CdSe nanocrystals with core composition of $(CdSe)_n$ [n = 29-36], as determined from LDI-MS analysis. The time-dependent characterization by absorption spectroscopic together with LDI-MS analysis showed that initially $(CdSe)_{19}$ nanocrystals were formed in the reaction mixture. Then the use of thermal driving force for destabilization resulted in monomeric species, which continuously attached onto existing CdSe nanocrystals in the process of formation of larger $(CdSe)_n$ nanocrystals (RNCs), while maintaining a diffusion-controlled growth mode. Our experimental results demonstrate the importance of the chemical nature of the chalcogenide precursors in the formation of MSNs as key intermediates, and we believe that this finding will lead to a better mechanistic understanding of group II-VI RNC synthesis and rational design of new synthetic protocols to prepare anisotropic nanostructures. It is expected that our mild reaction conditions will provide a more effective introduction methodology for transition metal doping during the growth of both MSN and RNCs allowing preparation of highly efficient nanomaterials for solid-state device fabrication.

The surface structure of the resulting nanocrystals was found to be extremely important in tailoring their photophysical properties, where coating of the stoichiometric core with a

mixture of Z-type [$Cd(O_2CPh)_2$] and L-type ligand [NH_2-R_2] produced a cadmium rich surface and showed a pronounced 1S(e)-$2S_{3/2}$(h) excitonic transition. Furthermore, the mixed surface ligand coating passivated the nonradiative surface traps and provided a substantial PLQY of ~27%. Post-synthetic ligand exchange on OLA-coated CdSe nanocrystals with $Cd(O_2CPh)_2$ further increased the PLQY by nearly a factor of two. Mixed OLA- and $Cd(O_2CPh)_2$-capped CdSe nanocrystals showed fluorescence lifetime of ~90 ns, a significantly high value for such small nanocrystals, and is due to delocalization of the exciton wave function into the ligand monolayer. These white light-emitting CdSe nanocrystals can be used to fabricate solid-state lighting (Figure S11), and slight modification of surface ligand chemistry should allow high charge conductivity and mobility for efficient light-emitting diode application.

Experimental Section:

Materials. Cadmium oxide (CdO, 99.9%), cadmium benzoate, cadmium acetate dihydrate ($Cd(OAc)_2 \cdot 2H_2O$, 98%), benzoic anhydride (> 95%), oleylamine (OLA, 70%), decylamine (95%), 1-octadecene (1-ODE, 90%), 1-hexanethiol (HT, 95%), benzoic acid (BA, 99.5%), selenium (Se pellets, 99.99%), coumarin-30 (99%), 2,4,6-trimethylstyrene (95%), toluene (HPLC, 99.9%), acetone (ACS reagent, 99.5%), acetonitrile (HPLC, 99.9%), and dichloromethane (ACS reagent, 99.5%) were purchased from Sigma-Aldrich. All chemicals were used as received without any further purification. The $Cd(benzoate)_2$ was synthesized according to a previously published procedure with modification.[31]

Spectroscopy and Spectrometry Characterization. UV-vis absorption spectra were collected using a Varian Cary 50 UV-vis spectrophotometer scanning through a range of 800-300 nm. Prior to the sample measurements, the baseline was corrected with pure solvent. The

photoluminescence emission (PL) spectra were acquired using a Cary Eclipse fluorescence spectrophotometer from Varian Instruments. The values of PLQY of the OLA- and BA/OLA-coated CdSe nanocrystals were calculated via a comparison technique using Coumarin 30 as a standard. Coumarin 30 displays its UV-vis absorption peak at 407 nm, and when excited at 380 nm it emits at 482 nm with a QY of 55.3% in acetonitrile.[76] All samples were prepared in toluene and the optical densities of the samples were kept to similar levels (~0.08-0.1). The emission data were collected from 400 nm to 700 nm. Eq. 1 was used to calculate the QY of the CdSe nanocrystals.

$$QY_{NC} = \left(\frac{E_{NC}/A_{NC}}{E_{STD}/A_{STD}} \right) \times \left(\frac{\eta_{NC}}{\eta_{STD}} \right)^2 \times QY_{STD} \qquad (1)$$

Here QY_{NC}, A_{NC} and E_{NC} represent the calculated quantum yield, absorbance, and integrated emission intensity of the CdSe nanocrystals, respectively, and QY_{STD}, A_{STD}, and E_{STD} are values of the Coumarin 30 standard used. η_{NC} is the refractive index of toluene (1.496) and η_{STD} the refractive index of acetonitrile (1.344).

The stretch exponential equation (Eq. 2) was used to determine the excited state lifetime using a Time-correlated single photon counting (TCSPC) experimental set up. Here I(t) and I_0 are the PL intensities at time t and zero. β and τ are the dispersion factor and emission decay time, respectively. For the limiting case where β→1, a single exponential decay was achieved with a characteristic lifetime of τ.

$$I(t) = I_0 \quad \exp\left[-\left(\frac{t}{\tau} \right)^{\beta} \right] \qquad (2)$$

Preparation of Se-ODE-HT Precursor. The selenium precursor, which we defined as Se-ODE-HT, was prepared as follows. Into a 25 mL 2 neck round bottom flask fitted with a temperature probe, 0.24 g (3.03 mmol) of freshly ground selenium powder and 8.0 mL (80 mmol) 1-ODE were transferred and kept under high vacuum for 30 min. This mixture was degassed and the container then filled with Ar. Next 0.43 mL (3.03 mmol) HT was injected through a syringe. The round bottom flask was then submerged in a pre-heated oil-bath at 160 °C with constant stirring for one hour until all of selenium powder dissolved yielding a light-yellow solution. The solution was removed from heat and cooled to room temperature. The Se-ODE-HT precursor when stored under inert atmosphere was stable for at least 4 days without any noticeable loss of its reactivity. A selenium precursor with identical reactivity in the CdSe nanocrystal formation can be prepared even as low as 150 °C, but required at least 6 hrs of heating.

Synthesis and Purification of White Light-Emitting CdSe(OLA) Nanocrystals. Into as-prepared Cd(acetate)$_2$-OLA precursor (see Supporting Information for detail), 2.0 mL of Se-ODE-HT solution was swiftly injected while stirring at room temperature under positive pressure of Ar. The light yellow color of ODE-Se-HT vanished immediately indicating rapid reaction between the cadmium and selenium precursors. After an approximately 1 h of stirring at room temperature, the reaction vessel was transferred to an oil-bath at 60 °C and allowed to form RNCs until a stable absorption peak at ~410 nm was obtained. During the stirring at 60 °C, the reaction mixture slowly turned from colorless to light yellow and finally bright yellow. The final CdSe nanocrystal solution was diluted with 20 mL of toluene and was clear and bright-yellow. Next, approximately 50 mL of acetone was added to form a turbid solution, which was centrifuged, and then the yellow solid was collected. The toluene dispersion and acetone precipitation step was repeated for an additional two times and the solid was dried under

vacuum. The bright yellow solid was stored in the dark and under Ar atmosphere prior to spectroscopy, spectrometry, and microscopy characterization.

Synthesis and Purification of CdSe(BA/OLA) Nanocrystals. A 2.0 mL, freshly prepared ODE-Se-HT solution was slowly injected into the Cd(benzoate)$_2$-OLA precursor at room temperature while stirring under Ar atmosphere. The experimental conditions for synthesis and purification were identical to those described for CdSe(OLA) nanocrystal synthesis.

ASSOCIATED CONTENT

Supporting Information. TEM images, additional UV-visible, PL, ^{1}H NMR and FT-IR, and MS spectra, additional experimental details, and additional discussion. This material is available free of charge via the Internet at http://pubs.acs.org.

AUTHOR INFORMATION

Corresponding Author

*Email: rsardar@iupui.edu

Author Contributions

The manuscript was written with contributions of all authors. All authors have given approval of the final version of the manuscript.

ACKNOWLEDGMENT

This work was supported by Indiana University-Purdue University Indianapolis start-up funds. We would like to thank Dr. Carrie Donley at UNC-Chapel Hill for the XPS analysis. EDS analyses were conducted with a Hitachi instrument purchased using funds from an NSF-MRI grant (MRI-1229514). The Bruker 500 MHz NMR was purchased using funds from an NSF-MRI award (CHE-0619254).

References:

(1) Klimov, V. I.; Mikhailovsky, A. A.; Xu, S.; Malko, A.; Hollingsworth, J. A.; Leatherdale, C. A.; Eisler, H.-J.; Bawendi, M. G. *Science* **2000**, *290*, 314-317.

(2) Huynh, W. U.; Dittmer, J. J.; Alivisatos, A. P. *Science* **2002**, *295*, 2425-2427.

(3) Gur, I.; Fromer, N. A.; Geier, M. L.; Alivisatos, A. P. *Science* **2005**, *310*, 462-465.

(4) Fleischhaker, F.; Zentel, R. *Chem. Mater.* **2005**, *17*, 1346-1351.

(5) Achermann, M.; Petruska, M. A.; Koleske, D. D.; Crawford, M. H.; Klimov, V. I. *Nano Lett.* **2006**, *6*, 1396-1400.

(6) Lim, J.; Jun, S.; Jang, E.; Baik, H.; Kim, H.; Cho, J. *Advanced Materials* **2007**, *19*, 1927-1932.

(7) Colvin, V. L.; Schlamp, M. C.; Alivisatos, A. P. *Nature* **1994**, *370*, 354-357.

(8) Coe, S.; Woo, W. K.; Bawendi, M.; Bulovic, V. *Nature* **2002**, *420*, 800-803.

(9) Talapin, D. V.; Lee, J.-S.; Kovalenko, M. V.; Shevchenko, E. V. *Chem. Rev.* **2009**, *110*, 389-458.

(10) Garcia-Rodriguez, R.; Hendricks, M. P.; Cossairt, B. M.; Liu, H.; Owen, J. S. *Chem. Mater.* **2013**, *25*, 1233-1249.

(11) Sowers, K. L.; Swartz, B.; Krauss, T. D. *Chem. Mater.* **2013**, *25*, 1351-1362.

(12) Newton, J. C.; Ramasamy, K.; Mandal, M.; Joshi, G. K.; Kumbhar, A.; Sardar, R. *J. Phys. Chem. C* **2012**, *116*, 4380-4389.

(13) Liu, H.; Owen, J. S.; Alivisatos, A. P. *J. Am. Chem. Soc.* **2006**, *129*, 305-312.

(14) Owen, J. S.; Chan, E. M.; Liu, H.; Alivisatos, A. P. *J. Am. Chem. Soc.* **2010**, *132*, 18206-18213.

(15) Peng, X. *Ad. Mater.* **2003**, *15*, 459-463.

(16) Harrell, S. M.; McBride, J. R.; Rosenthal, S. J. *Chem. Mater.* **2013**, *25*, 1199-1210.

(17) Kim, B. H.; Hackett, M. J.; Park, J.; Hyeon, T. *Chem. Mater.* **2013**, *26*, 59-71.

(18) Peng, Z. A.; Peng, X. *J. Am. Chem. Soc.* **2000**, *123*, 183-184.

(19) Son, J. S.; Wen, X.-D.; Joo, J.; Chae, J.; Baek, S.-i.; Park, K.; Kim, J. H.; An, K.; Yu, J. H.; Kwon, S. G.; Choi, S.-H.; Wang, Z.; Kim, Y.-W.; Kuk, Y.; Hoffmann, R.; Hyeon, T. *Angew. Chem. Int. Ed.* **2009**, *48*, 6861-6864.

(20) Ithurria, S.; Dubertret, B. *J. Am. Chem. Soc.* **2008**, *130*, 16504-16505.

(21) Liu, Y.-H.; Wang, F.; Wang, Y.; Gibbons, P. C.; Buhro, W. E. *J. Am. Chem. Soc.* **2011**, *133*, 17005-17013.

(22) Kilina, S.; Velizhanin, K. A.; Ivanov, S.; Prezhdo, O. V.; Tretiak, S. *ACS Nano* **2012**, *6*, 6515-6524.

(23) Long, R.; English, N. J.; Prezhdo, O. V. *J. Am. Chem. Soc.* **2013**, *135*, 18892-18900.

(24) Yang, Y.; Rodríguez-Córdoba, W.; Lian, T. *J. Am. Chem. Soc.* **2011**, *133*, 9246-9249.

(25) Yu, K. *Adv. Mater.* **2012**, *24*, 1123-1132.

(26) Bowers, M. J.; McBride, J. R.; Rosenthal, S. J. *J. Am. Chem. Soc.* **2005**, *127*, 15378-15379.

(27) Evans, C. M.; Guo, L.; Peterson, J. J.; Maccagnano-Zacher, S.; Krauss, T. D. *Nano Lett.* **2008**, *8*, 2896-2899.

(28) Kudera, S.; Zanella, M.; Giannini, C.; Rizzo, A.; Li, Y.; Gigli, G.; Cingolani, R.; Ciccarella, G.; Spahl, W.; Parak, W. J.; Manna, L. *Adv. Mater.* **2007**, *19*, 548-552.

(29) Cossairt, B. M.; Owen, J. S. *Chem. Mater.* **2011**, *23*, 3114-3119.

(30) Wang, Y.; Zhang, Y.; Wang, F.; Giblin, D. E.; Hoy, J.; Rohrs, H. W.; Loomis, R. A.; Buhro, W. E. *Chem. Mater.* **2014**, *26*, 2233-2243.

(31) Beecher, A. N.; Yang, X.; Palmer, J. H.; LaGrassa, A. L.; Juhas, P.; Billinge, S. J. L.; Owen, J. S. *J. Am. Chem. Soc.* **2014**, *136*, 10645-10653.

(32) Dukes, A. D.; McBride, J. R.; Rosenthal, S. J. *Chem. Mater.* **2010**, *22*, 6402-6408.

(33) Dukes, A. D.; Iii; Schreuder, M. A.; Sammons, J. A.; McBride, J. R.; Smith, N. J.; Rosenthal, S. J. *J. Chem. Phys.* **2008**, *129*, 121102-121104.

(34) Rosson, T. E.; Claiborne, S. M.; McBride, J. R.; Stratton, B. S.; Rosenthal, S. J. *J. Am. Chem. Soc.* **2012**, *134*, 8006-8009.

(35) Krause, M. M.; Mooney, J.; Kambhampati, P. *ACS Nano* **2013**, *7*, 5922-5929.

(36) Landes, C. F.; Braun, M.; El-Sayed, M. A. *J. Phys. Chem. B* **2001**, *105*, 10554-10558.

(37) Bowers Ii, M. J.; McBride, J. R.; Garrett, M. D.; Sammons, J. A.; Dukes Iii, A. D.; Schreuder, M. A.; Watt, T. L.; Lupini, A. R.; Pennycook, S. J.; Rosenthal, S. J. *J. Am. Chem. Soc.* **2009**, *131*, 5730-5731.

(38) Schreuder, M. A.; Xiao, K.; Ivanov, I. N.; Weiss, S. M.; Rosenthal, S. J. *Nano Lett.* **2010**, *10*, 573-576.

(39) Bullen, C.; van Embden, J.; Jasieniak, J.; Cosgriff, J. E.; Mulder, R. J.; Rizzardo, E.; Gu, M.; Raston, C. L. *Chem. Mater.* **2010**, *22*, 4135-4143.

(40) Bullen, C. R.; Mulvaney, P. *Nano Lett.* **2004**, *4*, 2303-2307.

(41) Dolai, S.; Nimmala, P. R.; Mandal, M.; Muhoberac, B. B.; Dria, K.; Dass, A.; Sardar, R. *Chem. Mater.* **2014**, *26*, 1278-1285.

(42) Dolai, S.; Dass, A.; Sardar, R. *Langmuir* **2013**, *29*, 6187-6193.

(43) Steigerwald, M. L.; Brus, L. E. *Acc. Chem. Res.* **1990**, *23*, 183–188.

(44) Chen, O.; Yang, Y.; Wang, T.; Wu, H.; Niu, C.; Yang, J.; Cao, Y. C. *J. Am. Chem. Soc.* **2011**, *133*, 17504-17512.

(45) Morris-Cohen, A. J.; Frederick, M. T.; Lilly, G. D.; McArthur, E. A.; Weiss, E. A. *J. Phys. Chem. Lett.* **2010**, *1*, 1078–1081.

(46) Fritzinger, B.; Capek, R. K.; Lambert, K.; Martins, J. C.; Hens, Z. *J. Am. Chem. Soc.* **2010**, *132*, 10195-10201.

(47) Hassinen, A.; Moreels, I.; De Nolf, K.; Smet, P. F.; Martins, J. C.; Hens, Z. *J. Am. Chem. Soc.* **2012**, *134*, 20705-20712.

(48) Li, Z.; Peng, X. *J. Am. Chem. Soc.* **2011**, *133*, 6578-6586.

(49) Owen, J. S.; Park, J.; Trudeau, P.-E.; Alivisatos, A. P. *J. Am. Chem. Soc.* **2008**, *130*, 12279-12281.

(50) Cossairt, B. M.; Juhas, P.; Billinge, S. J. L.; Owen, J. S. *J. Phys. Chem. Lett.* **2011**, *2*, 3075-3080.

(51) Murray, C. B.; Norris, D. J.; Bawendi, M. G. *J. Am. Chem. Soc.* **1993**, *115*, 8706-8715.

(52) Yang, Y. A.; Wu, H.; Williams, K. R.; Cao, Y. C. *Angew. Chem. Int. Ed.* **2005**, *44*, 6712-6715.

(53) Peng, X.; Wickham, J.; Alivisatos, A. P. *J. Am. Chem. Soc.* **1998**, *120*, 5343-5344.

(54) Talapin, D. V.; Rogach, A. L.; Kornowski, A.; Haase, M.; Weller, H. *Nano Lett.* **2001**, *1*, 207-211.

(55) Peng, Z. A.; Peng, X. *J. Am. Chem. Soc.* **2001**, *123*, 1389-1395.

(56) Evans, C. M.; Love, A. M.; Weiss, E. A. *J. Am. Chem. Soc.* **2012**, *134*, 17298-17305.

(57) Park, Y.-S.; Dmytruk, A.; Dmitruk, I.; Kasuya, A.; Okamoto, Y.; Kaji, N.; Tokeshi, M.; Baba, Y. *J. Phys. Chem. C* **2010**, *114*, 18834-18840.

(58) Del Ben, M.; Havenith, R. W. A.; Broer, R.; Stener, M. *J. Phys. Chem. C* **2011**, *115*, 16782-16796.

(59) Talapin, D. V.; Rogach, A. L.; Shevchenko, E. V.; Kornowski, A.; Haase, M.; Weller, H. *J. Am. Chem. Soc.* **2002**, *124*, 5782-5790.

(60) Wang, Y.; Liu, Y.-H.; Zhang, Y.; Wang, F.; Kowalski, P. J.; Rohrs, H. W.; Loomis, R. A.; Gross, M. L.; Buhro, W. E. *Angew. Chem. Int. Ed.* **2012**, *51*, 6154-6157.

(61) Wang, Y.; Zhang, Y.; Wang, F.; Giblin, D. E.; Hoy, J.; Rohrs, H. W.; Loomis, R. A.; Buhro, W. E. *Chem. Mater.* **2014**, *26*, 2233-2243.

(62) Jose, R.; Zhanpeisov, N. U.; Fukumura, H.; Baba, Y.; Ishikawa, M. *J. Am. Chem. Soc.* **2005**, *128*, 629-636.

(63) Kasuya, A.; Sivamohan, R.; Barnakov, Y. A.; Dmitruk, I. M.; Nirasawa, T.; Romanyuk, V. R.; Kumar, V.; Mamykin, S. V.; Tohji, K.; Jeyadevan, B.; Shinoda, K.; Kudo, T.; Terasaki, O.; Liu, Z.; Belosludov, R. V.; Sundararajan, V.; Kawazoe, Y. *Nat. Mater.* **2004**, *3*, 99-102.

(64) Peng, Z. A.; Peng, X. *J. Am. Chem. Soc.* **2002**, *124*, 3343-3353.

(65) Cumberland, S. L.; Hanif, K. M.; Javier, A.; Khitrov, G. A.; Strouse, G. F.; Woessner, S. M.; Yun, C. S. *Chem. Mater.* **2002**, *14*, 1576-1584.

(66) Evans, C. M.; Evans, M. E.; Krauss, T. D. *J. Am. Chem. Soc.* **2010**, *132*, 10973-10975.

(67) Garcia-Rodriguez, R.; Liu, H. *J. Am. Chem. Soc.* **2012**, *134*, 1400-1403.

(68) Steckel, J. S.; Yen, B. K. H.; Oertel, D. C.; Bawendi, M. G. *J. Am. Chem. Soc.* **2006**, *128*, 13032-13033.

(69) Chen, O.; Chen, X.; Yang, Y.; Lynch, J.; Wu, H.; Zhuang, J.; Cao, Y. C. *Angew. Chem. Int. Ed.* **2008**, *47*, 8638-8641.

(70) Cao, Y. C.; Wang, J. *J. Am. Chem. Soc.* **2004**, *126*, 14336-14337.

(71) Jasieniak, J.; Mulvaney, P. *J. Am. Chem. Soc.* **2007**, *129*, 2841-2848.

(72) Shen, H.; Wang, H.; Li, X.; Niu, J. Z.; Wang, H.; Chen, X.; Li, L. S. *Dalton Trans.* **2009**, 10534-10540.

(73) Demko, B. A.; Wasylishen, R. E. *Prog. Nucl. Magn. Reson. Spectrosc.* **2009**, *54*, 208-238.

(74) Liu, Y.; Yao, D.; Shen, L.; Zhang, H.; Zhang, X.; Yang, B. *J. Am. Chem. Soc.* **2012**, *134*, 7207-7210.

(75) Riehle, F. S.; Bienert, R.; Thomann, R.; Urban, G. A.; Kruger, M. *Nano Lett.* **2009**, *9*, 514-518.

(76) Senthilkumar, S.; Nath, S.; Pal, H. *Photochem. and Photobiol.* **2004**, *80*, 104-111.

(77) Anderson, N. C.; Hendricks, M. P.; Choi, J. J.; Owen, J. S. *J. Am. Chem. Soc.* **2013**, *135*, 18536-18548.

(78) Lee, H.; Holloway, P. H.; Yang, H.; Hardison, L.; Kleiman, V. D. *J. Chem Phys.* **2006**, *125*, 164711-164716.
(79) Mokari, T.; Banin, U. *Chem. Mater.* **2003**, *15*, 3955-3960.
(80) Frederick, M. T.; Weiss, E. A. *ACS Nano* **2010**, *4*, 3195-3200.
(81) Teunis, M. B.; Dolai, S.; Sardar, R. *Langmuir* **2014**, *30*, 7851-7858.
(82) Kuçur, E.; Ziegler, J.; Nann, T. *Small* **2008**, *4*, 883-887.
(83) Peng, H.-C.; Kang, C.-C.; Liang, M.-R.; Chen, C.-Y.; Demchenko, A.; Chen, C.-T.; Chou, P.-T. *ACS Appl. Mater. Interfaces* **2011**, *3*, 1713-1720.
(84) Khitrov, G. A.; Strouse, G. F. *J. Am. Chem. Soc.* **2003**, *125*, 10465-10469.
(85) Hunter, J. M.; Lin, H.; Becker, C. H. *Anal. Chem.* **1997**, *69*, 3608-3612.
(86) Jungbauer, L. M.; Cavagnero, S. *Anal. Chem.* **2006**, *78*, 2841-2852.
(87) Dass, A.; Stevenson, A.; Dubay, G. R.; Tracy, J. B.; Murray, R. W. *J. Am. Chem. Soc.* **2008**, *130*, 5940-5946.
(88) Qian, H.; Zhu, Y.; Jin, R. *Procc. Natl. Acad. Sci.* **2012**.
(89) Yu, W. W.; Qu, L.; Guo, W.; Peng, X. *Chem. Mater.* **2003**, *15*, 2854-2860.
(90) Fisher, B. R.; Eisler, H.-J.; Stott, N. E.; Bawendi, M. G. *J. Phys. Chem. B* **2003**, *108*, 143-148.

List of Schemes and Figures

Scheme 1. The Reaction Pathway of Phosphine-Free Synthesis of Ultra-Bright White Light-Emitting ~1.6 nm CdSe Nanocrystals using Cd- and Se-containing precursors[a]

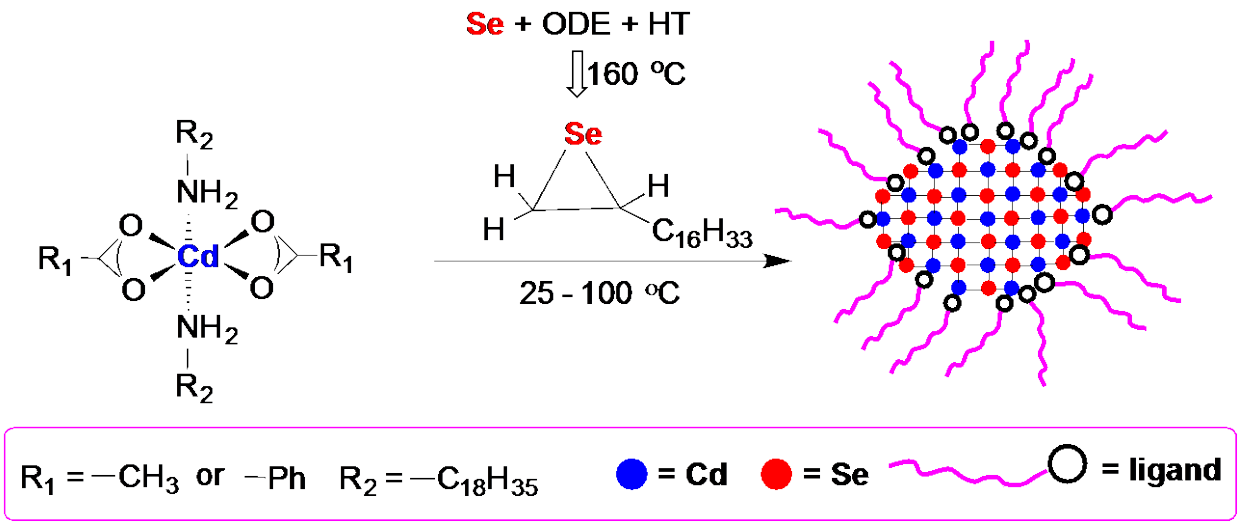

[a]CdSe nanocrystals were synthesized with either oleylamine or mixed ligation of benzoate (BA, -O_2C-Ph) and oleylamine (OLA, NH_2-R_2). The average lattice core was determined to be $(CdSe)_{33}$ by laser desorption ionization-mass spectrometry. For simplicity no specific surface ligands are illustrated here.

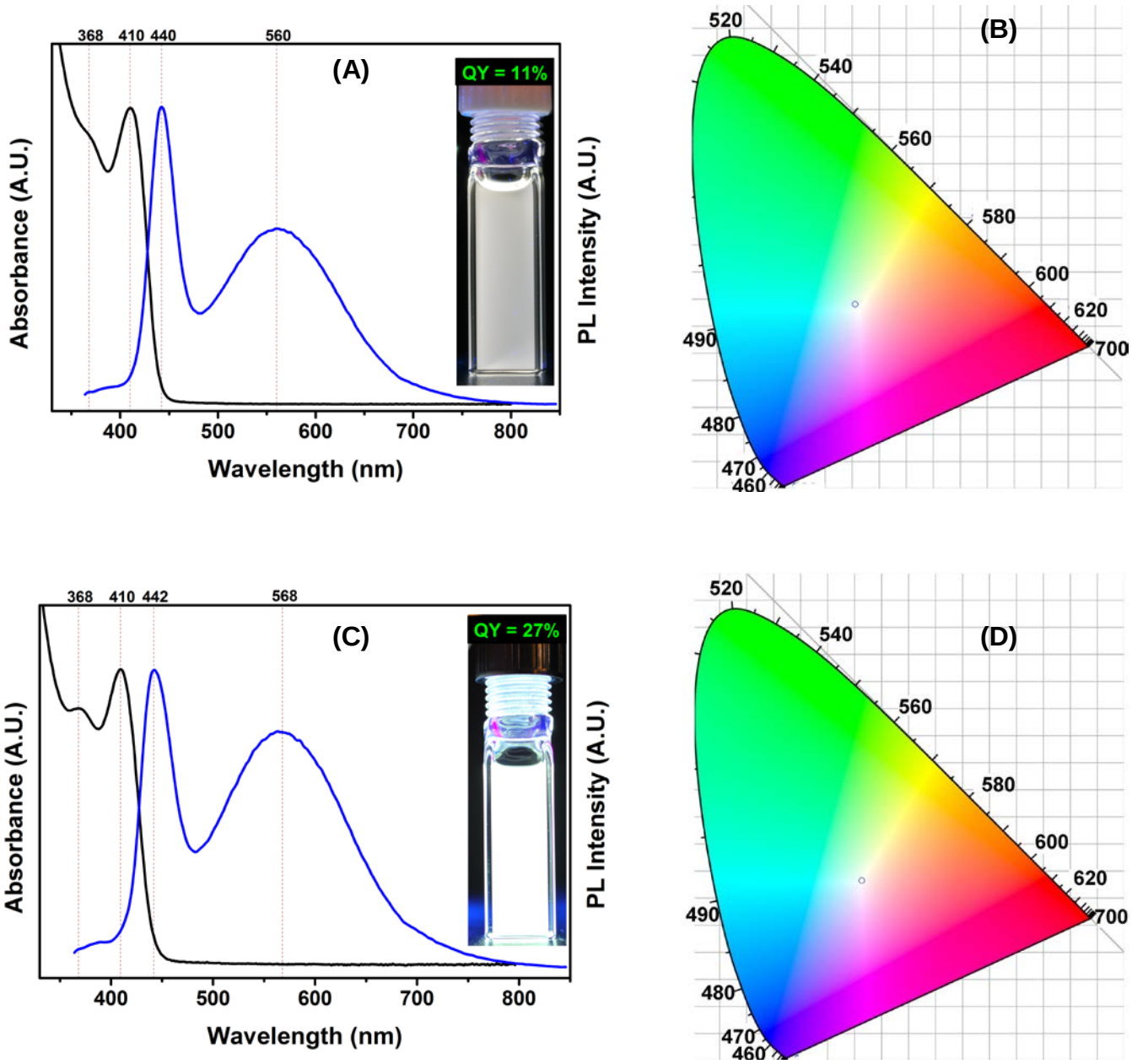

Figure 1. (A) UV-vis absorption (black) and PL (blue) of CdSe(OLA) nanocrystals. Insert shows white-light emitting nanocrystals under illumination of UV light. (B) Internationale d'Eclairage chromaticity coordinates (x = 0.310, y = 0.316) of CdSe(OLA) nanocrystals. (C) UV-vis absorption (black) and PL (blue) of CdSe(BA/OLA) nanocrystals. Insert shows white-light emitting nanocrystals under illumination of UV light. (D) CIE coordinates (x = 0.330, y = 0.337) of CdSe(BA/OLA) nanocrystals.

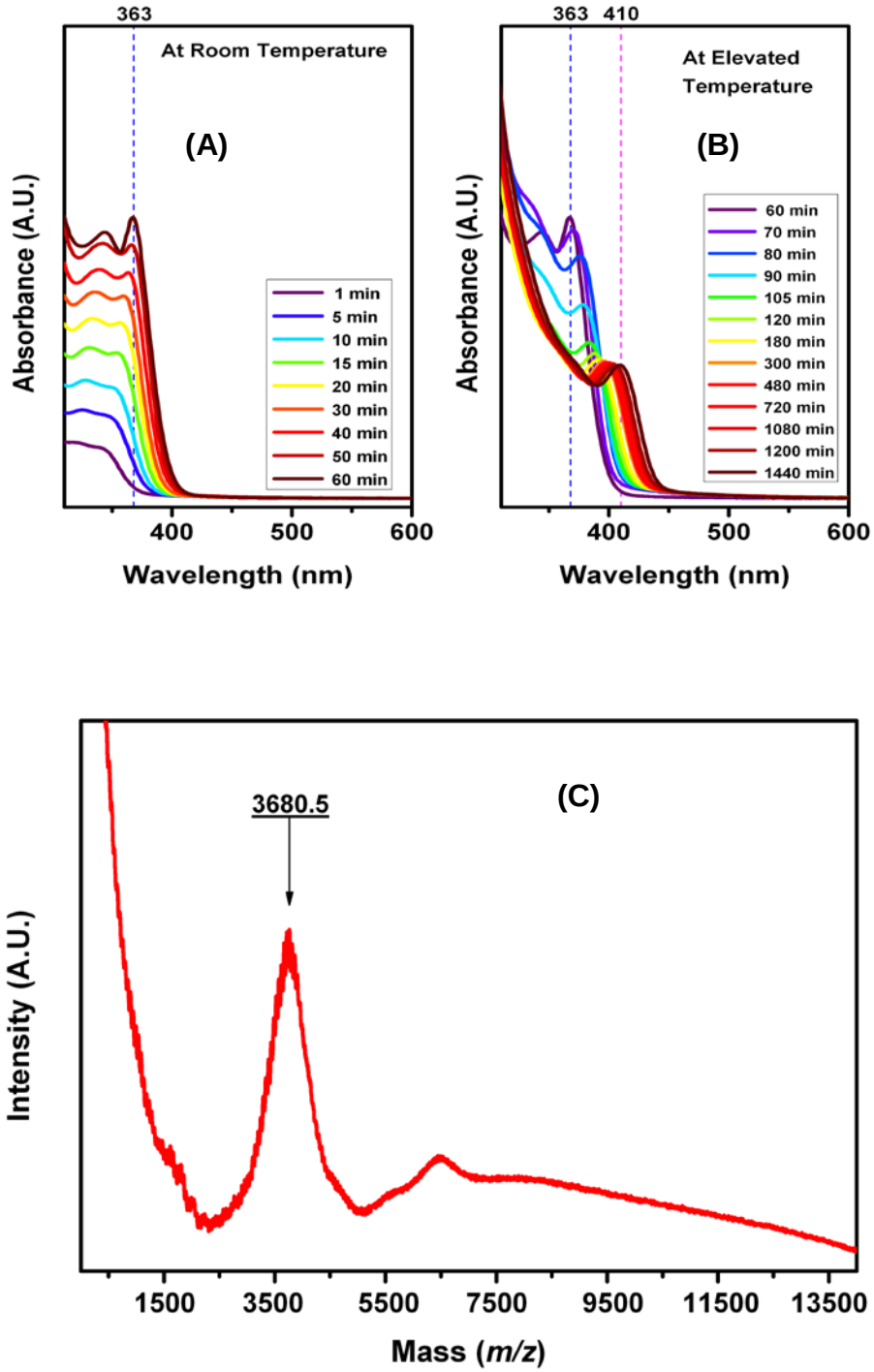

Figure 2. (A) Time dependent UV-vis absorption spectra of CdSe nanocrystal formation from the reaction between Cd-OLA and the Se-ODE-HT precursor at room temperature. The band edge peak at 363 nm implies existence of $(CdSe)_{19}$ nanocrystals in the reaction mixture. (B) Time dependent UV-vis absorption spectra of CdSe nanocrystal formation after heating the $(CdSe)_{19}$ nanocrystal reaction mixture at 60 ^{o}C over a period of 24 h. (C) Positive mode LDI-MS spectrum of $(CdSe)_{19}$ nanocrystals after 60 min of reaction at room temperature.

Scheme 2. Diagram showing steps from initial formation of monomers to $(CdSe)_{19}$ nanocrystals and then continuous size evolution through attachment of monomer to the growing nanocrystals

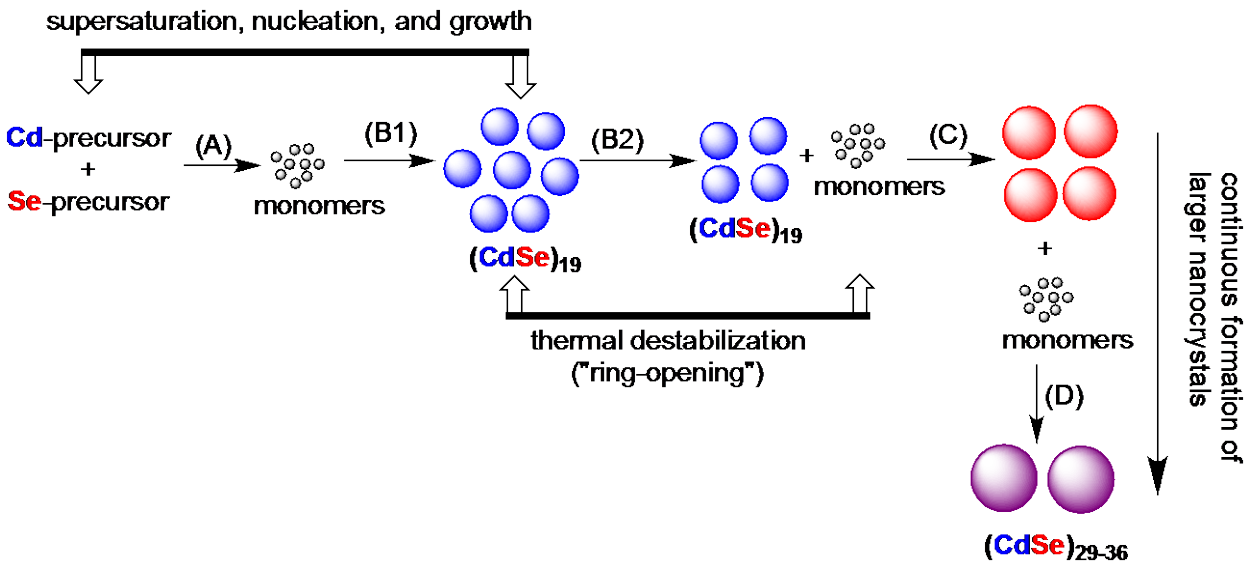

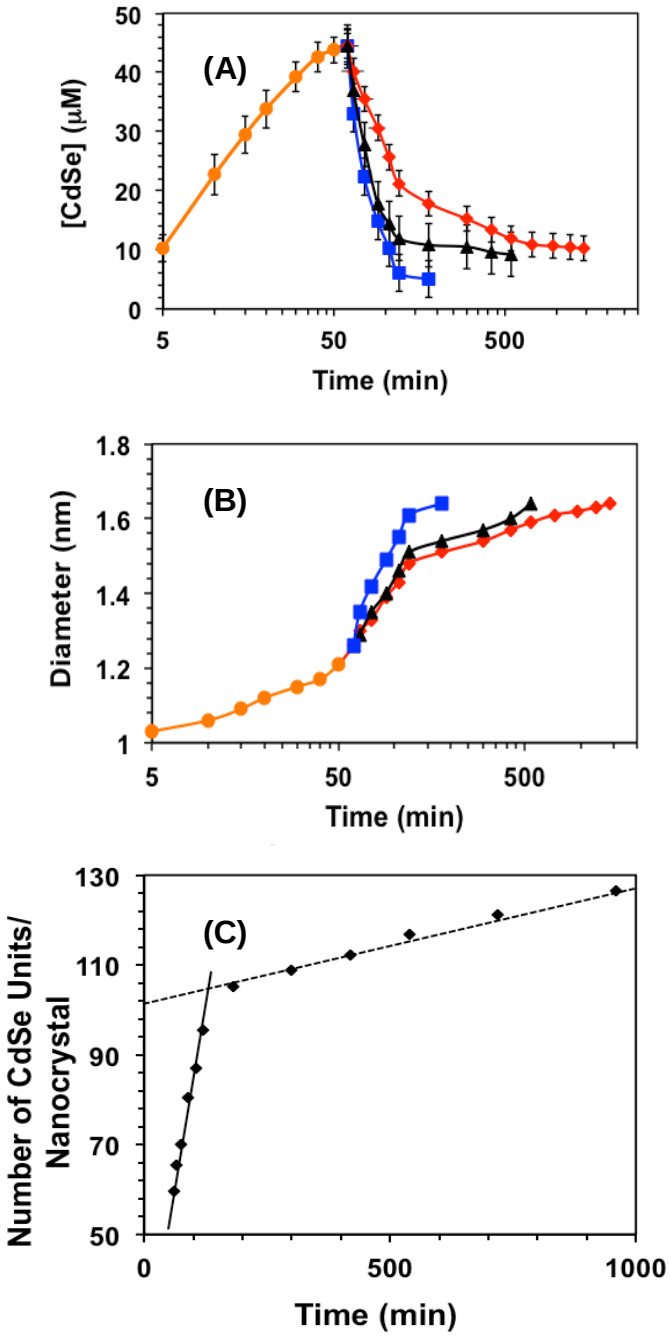

Figure 3. (A) Overall changes in CdSe nanocrystal concentration and (B) average diameter with time for the reaction between Cd-OLA and Se-ODE-HT precursors at different temperatures: room temperature (●), 60 ºC (◆), 80 ºC (▲), and 100 ºC (■). Both concentration and diameter were calculated from an empirical formula based on UV-vis absorption peak position.[89] (C) The average number of CdSe units per nanocrystal at different times was calculated from graph A (lower panel). The solid straight line with larger positive slope represents continuous size evolution while maintaining size monodispersity as an example of the living polymerization mechanism.

Scheme 3. Reaction Pathways for the Formation of Different Organometallic Species Containing Selenium.

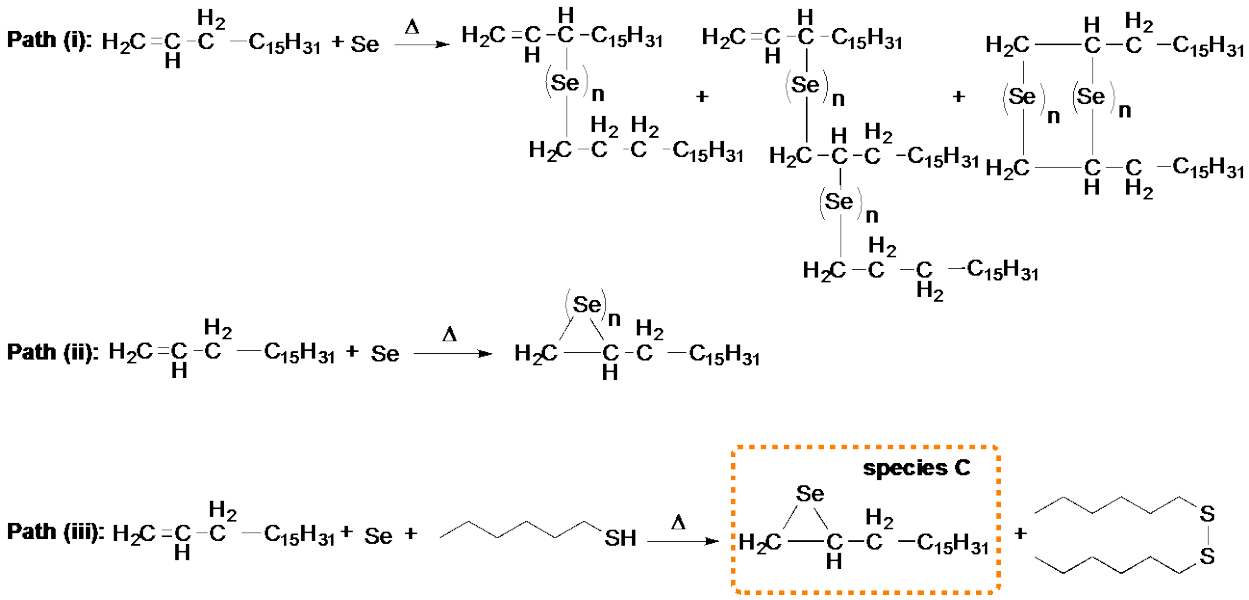

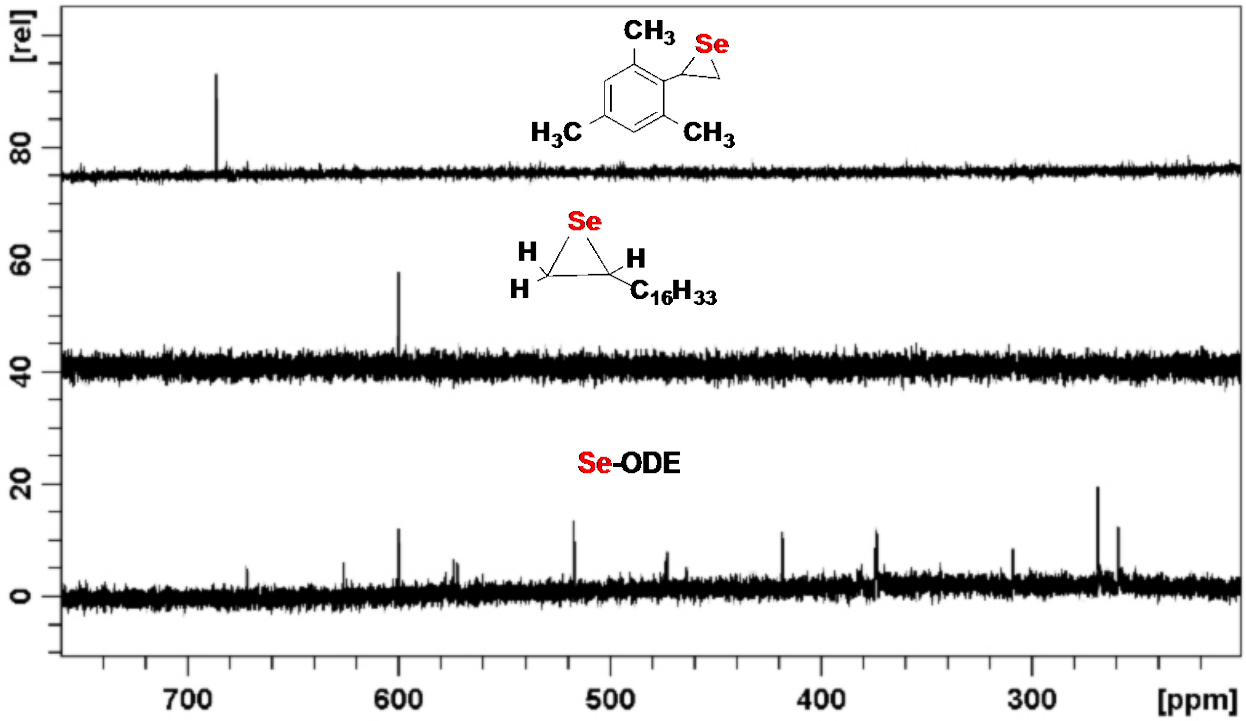

Figure 4. ^{77}Se NMR spectra of different selenium precursors. Top, middle, and bottom panels represent selenium precursor prepared from elemental selenium with 2,4,6-trimethylstyrene and hexanethiol, selenium with 1-octadecene (ODE) and hexanethiol, and selenium with 1-octadecene, respectively. Ph_2Se_2 was used as an internal standard. All spectra were collected in $CDCl_3$.

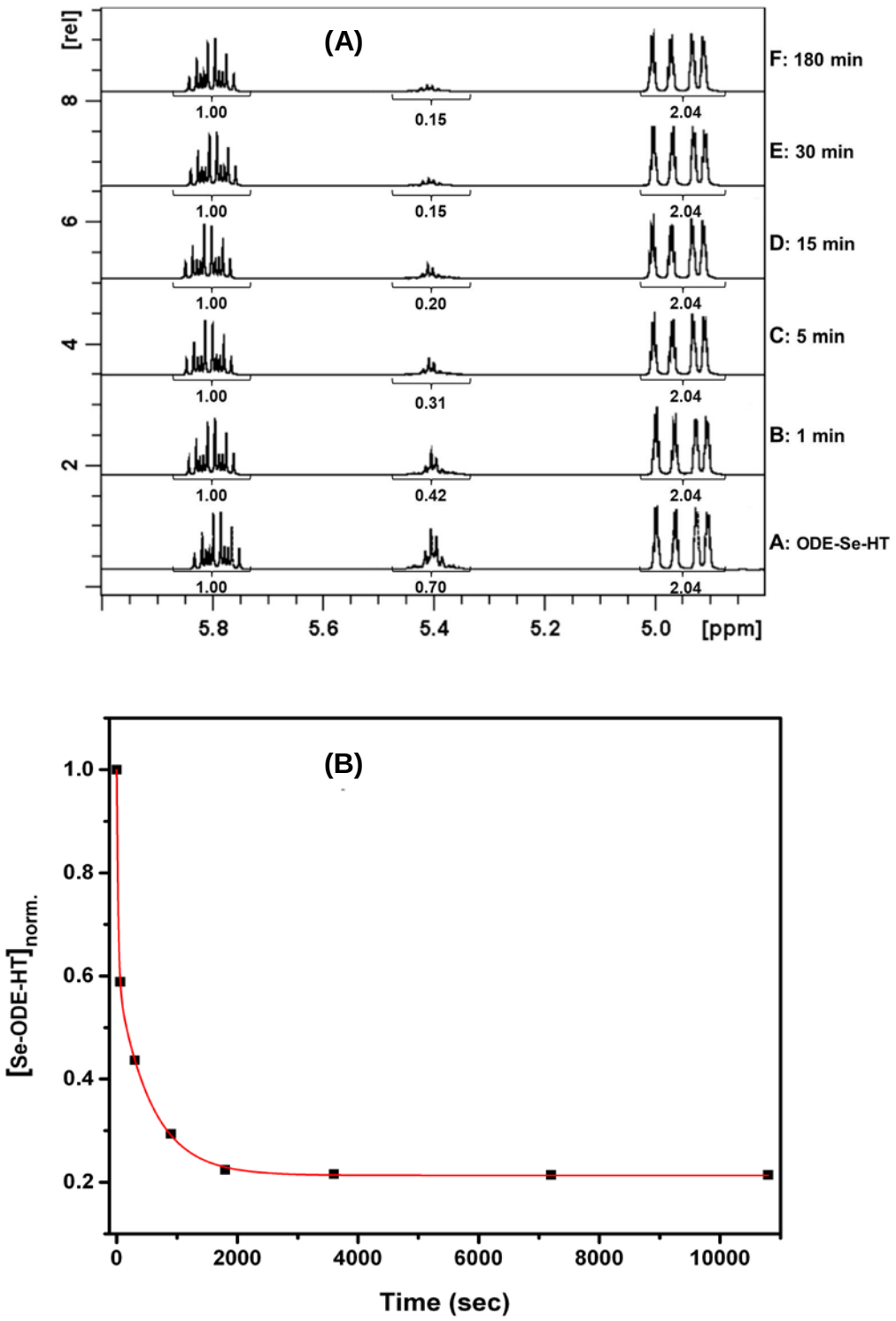

Figure 5. (A) Time dependent ^{1}H NMR spectra of CdSe nanocrystal formation from the reaction between Cd-benzoate-decylamine precursor and Se-ODE-HT precursor. The presence of multiplets at 5.4 ppm signifies the formation of species C as described in Scheme 2, path (iii). (B) Single exponential fit to the disappearance of Se-ODE-HT during the formation of CdSe nanocrystals. The multiplet at 5.4 ppm was used to monitor the consumption of Se precursor during nanocrystal formation. The fit was a single-exponential decay and the corresponding rate of disappearance was $2.3 \pm 0.18 \times 10^{-4}$ s^{-1}.

Scheme 4. Proposed mechanism of selenium release from Se-bridged organic precursor during the generation of CdSe monomers and formation of CdSe nanocrystals

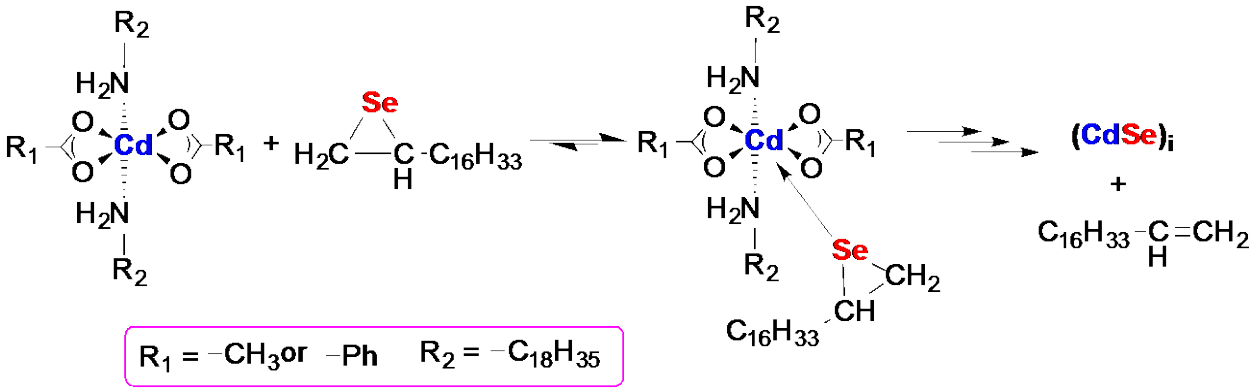

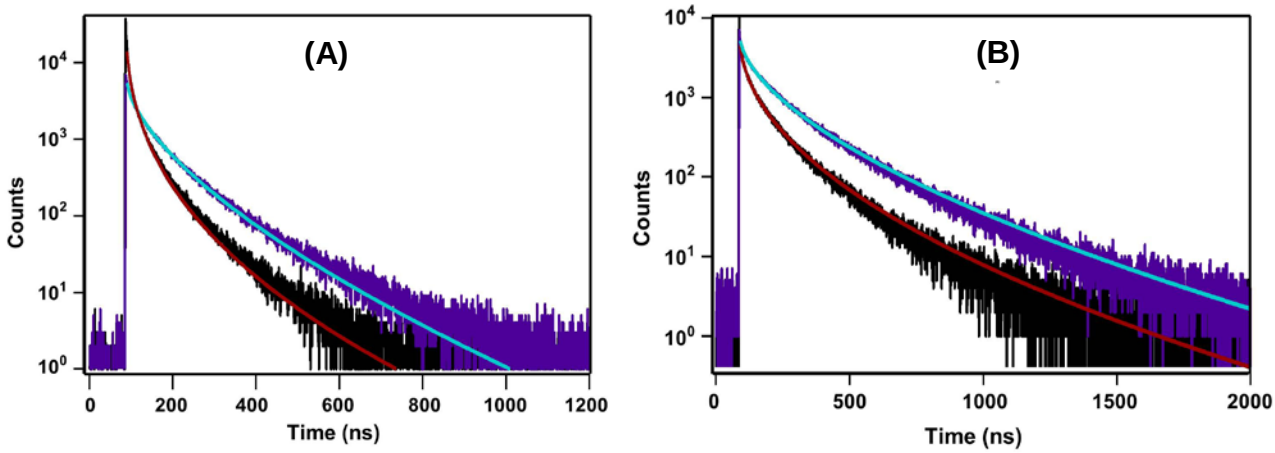

Figure 6. PL decay of CdSe(OLA) (A) and CdSe (BA/OLA) nanocrystals (B) excited at 405 nm. The light-blue and red curves represent the fit to the decay rates monitored at 550 and 440 nm. The stretch exponential equation (Eq. 2)[78,90] was used to determine the excited state lifetimes.

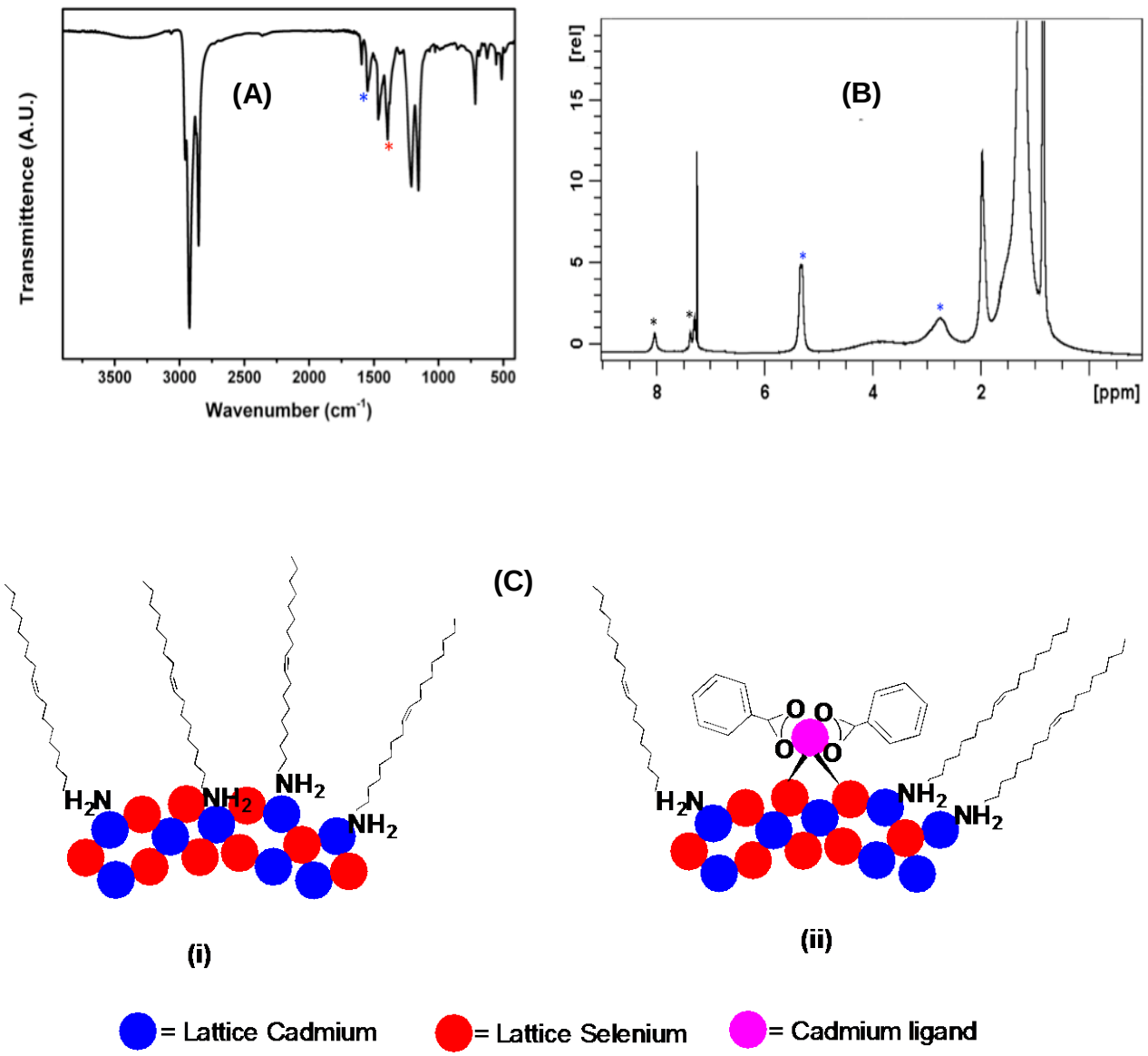

Figure 7. (A) FT-IR spectrum of CdSe(BA/OLA) nanocrystals where symmetric and anti-symmetric CO stretches are at 1387 (red asterisk) and 1543 cm^{-1} (blue asterisk), respectively. (B) ^{1}H NMR spectrum of CdSe(BA/OLA) nanocrystals where black and blue asterisks represent proton signals from BA and OLA hydrogens, respectively. The spectrum was collected in $CDCl_3$. (C) Surface ligand mode of binding for a stoichiometry core of CdSe nanocrystal with (i) only OLA and (ii) a mixture of OLA and $Cd(O_2CPh)_2$.

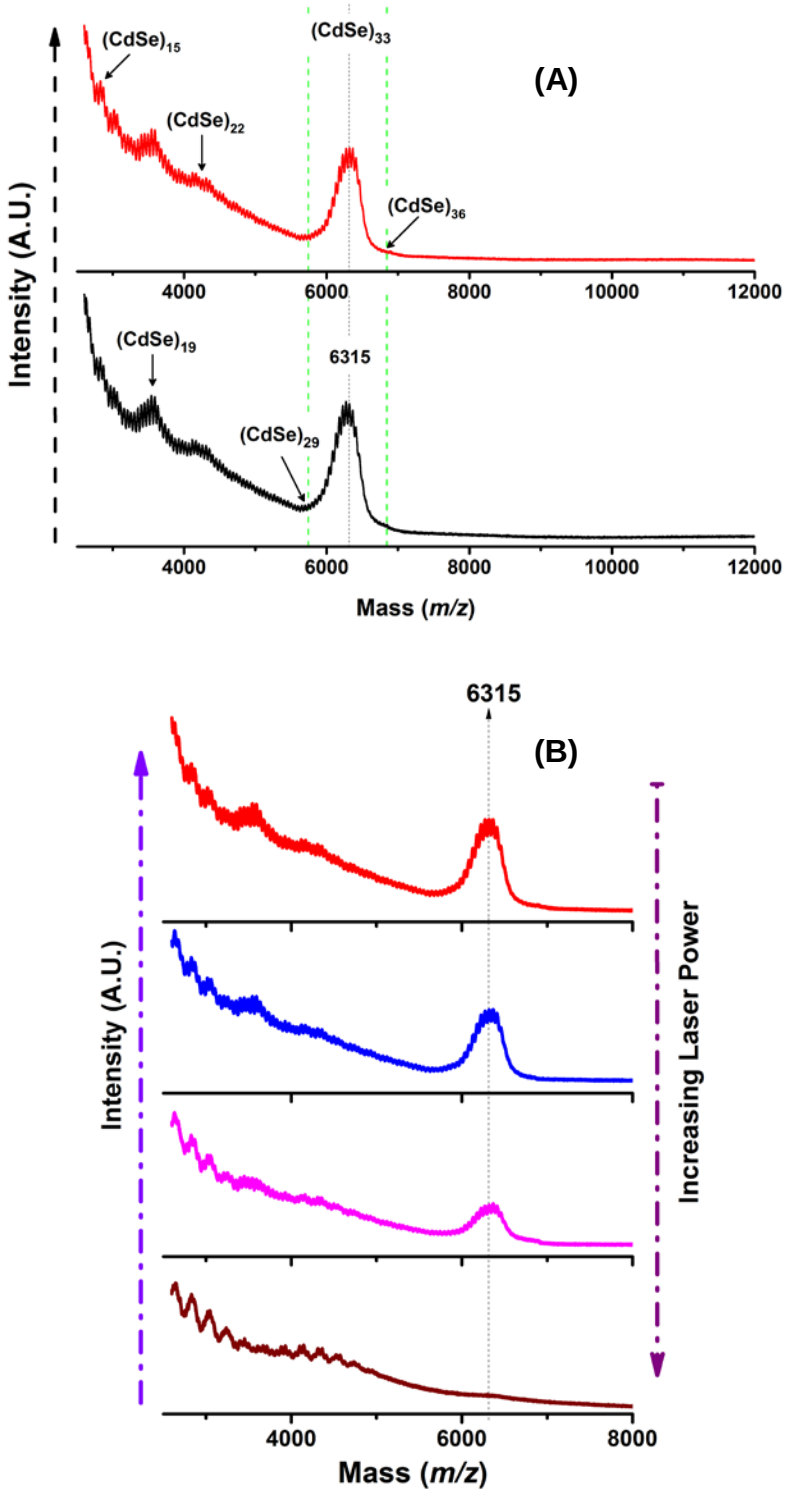

Figure 8. (A) Positive mode LDI-MS spectrum of OLA-coated (red) and mixed BA- and OLA-coated (black) CdSe nanocrystals. (B) Positive mode LSI-MS spectra of mixed BA- and OLA-coated CdSe nanocrystals with varying laser power to demonstrate the composition of the parent core mass of 6315 kDa.

TOC Graphic

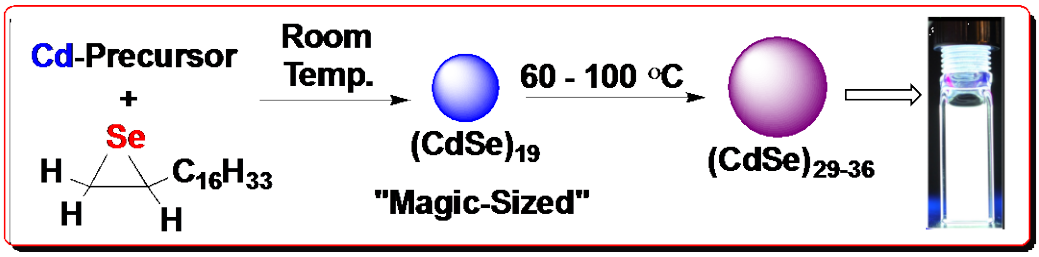
Cd-Precursor
+
Se
H
H
H
C16H33
Room
Temp.
(CdSe)19
"Magic-Sized"
60 - 100 °C
(CdSe)29-36